The Plant Cell, Vol. 29: 3012–3029, December 2017, www.plantcell.org © 2017 ASPB.

Arabidopsis Pollen Fertility Requires the Transcription Factors CITF1 and SPL7 That Regulate Copper Delivery to Anthers and Jasmonic Acid Synthesis[OPEN]

Jiapei Yan,[a,1] Ju-Chen Chia,[a,1] Huajin Sheng,[a] Ha-il Jung,[a] Tetiana-Olena Zavodna,[a] Lu Zhang,[a] Rong Huang,[b] Chen Jiao,[c] Eric J. Craft,[d] Zhangjun Fei,[c] Leon V. Kochian,[e] and Olena K. Vatamaniuk[a,2]

[a] Soil and Crop Sciences Section, School of Integrative Plant Science, Cornell University, Ithaca, New York 14853
[b] Cornell High Energy Synchrotron Source, Cornell University, Ithaca, New York 14853
[c] Boyce Thompson Institute for Plant Research, Ithaca, New York 14853
[d] Robert W. Holley Center for Agriculture and Health, U.S. Department of Agriculture-Agricultural Research Service, Ithaca, New York 14853-2901
[e] Global Institute for Food Security, University of Saskatchewan, Saskatoon S7N 5A8, Canada

ORCID IDs: 0000-0003-2573-2702 (J.Y.); 0000-0002-7498-5071 (J.-C.C.); 0000-0003-0215-4823 (R.H.); 0000-0001-9684-1450 (Z.F.); 0000-0003-3416-089X (L.V.K.); 0000-0003-2713-3797 (O.K.V.)

A deficiency of the micronutrient copper (Cu) leads to infertility and grain/seed yield reduction in plants. How Cu affects fertility, which reproductive structures require Cu, and which transcriptional networks coordinate Cu delivery to reproductive organs is poorly understood. Using RNA-seq analysis, we showed that the expression of a gene encoding a novel transcription factor, CITF1 (Cu-DEFICIENCY INDUCED TRANSCRIPTION FACTOR1), was strongly upregulated in *Arabidopsis thaliana* flowers subjected to Cu deficiency. We demonstrated that CITF1 regulates Cu uptake into roots and delivery to flowers and is required for normal plant growth under Cu deficiency. CITF1 acts together with a master regulator of copper homeostasis, SPL7 (SQUAMOSA PROMOTER BINDING PROTEIN LIKE7), and the function of both is required for Cu delivery to anthers and pollen fertility. We also found that Cu deficiency upregulates the expression of jasmonic acid (JA) biosynthetic genes in flowers and increases endogenous JA accumulation in leaves. These effects are controlled in part by CITF1 and SPL7. Finally, we show that JA regulates *CITF1* expression and that the JA biosynthetic mutant lacking the CITF1- and SPL7-regulated genes, *LOX3* and *LOX4*, is sensitive to Cu deficiency. Together, our data show that CITF1 and SPL7 regulate Cu uptake and delivery to anthers, thereby influencing fertility, and highlight the relationship between Cu homeostasis, CITF1, SPL7, and the JA metabolic pathway.

INTRODUCTION

Copper (Cu) is an essential micronutrient that is involved in important biological processes including respiration, photosynthesis, and scavenging of oxidative stress in all organisms (Ravet and Pilon, 2013; Broadley et al., 2012; Burkhead et al., 2009). In addition to these functions, plants require Cu for the perception of hormones, cell wall dynamics, and response to pathogens and reproduction (Shorrocks and Alloway, 1988; Ravet and Pilon, 2013; Mendel and Kruse, 2012; Printz et al., 2016; Broadley et al., 2012). Cu deficiency in humans is an increasingly recognized cause of anemia (Daughety and DeLoughery, 2017) and the dramatic consequences of imbalanced Cu homeostasis are known as Menkes and Wilson diseases (Llanos and Mercer, 2002). Among the visible symptoms of Cu deficiency in plants are stunted growth, chlorosis/necrosis of leaves, crop lodging, compromised fertility, and, in acute cases, total crop failure (Shorrocks and Alloway, 1988; Broadley et al., 2012). Cu deficiency in plants develops in alkaline soils that occupy ~30% of the world's arable land, and in organic soils (Shorrocks and Alloway, 1988; Broadley et al., 2012). While Cu deficiency can be remedied by the application of Cu-based fertilizers, this strategy is not environmentally friendly, and the repeated use of fertilizers as well as Cu-containing pesticides has led to the buildup of toxic levels of Cu in soils (Shorrocks and Alloway, 1988; Broadley et al., 2012). Organic farming has emerged as a production system that relies on natural fertilizers. However, natural fertilizers increase soil organic matter, further reducing Cu bioavailability in soils.

The remarkable array of physiological functions of Cu is attributed to its ability to change its oxidation state ($Cu^{2+} \leftrightarrow Cu^{+}$) (Ravet and Pilon, 2013; Broadley et al., 2012; Burkhead et al., 2009). However, the same chemical property can result in toxicity when free Cu ions accumulate in cells in excess because they promote oxidative stress (Burkhead et al., 2009). To maintain Cu homeostasis, plants regulate cellular Cu uptake and economize on Cu during deficiency (Ravet et al., 2011; Shahbaz et al., 2015; Burkhead et al., 2009). An uptake-based Cu homeostatic mechanism involves the upregulated expression of Cu acquisition and transport genes under Cu deficiency (Burkhead et al., 2009). The Cu economy or "metal switch" mechanism, originally discovered in

[1] These authors contributed equally to this work.
[2] Address correspondence to okv2@cornell.edu.
The author responsible for distribution of materials integral to the findings presented in this article in accordance with the policy described in the Instructions for Authors (www.plantcell.org) is: Olena K. Vatamaniuk (okv2@cornell.edu).
[OPEN] Articles can be viewed without a subscription.
www.plantcell.org/cgi/doi/10.1105/tpc.17.00363

the green alga *Chlamydomonas reinhardtii*, includes the down-regulation of the expression of potentially redundant Cu proteins for the metabolic reutilization of cellular Cu reserves (Burkhead et al., 2009; Blaby-Haas and Merchant, 2017; Kropat et al., 2015; Ravet et al., 2011; Shahbaz et al., 2015). In *Arabidopsis thaliana*, both processes are controlled by a conserved transcription factor, SPL7 (SQUAMOSA PROMOTER BINDING PROTEIN LIKE7), a homolog of the algal Cu sensor, CRR1 (COPPER RESPONSE REGULATOR1) (Yamasaki et al., 2009; Bernal et al., 2012; Garcia-Molina et al., 2014; Sommer et al., 2010; Kropat et al., 2005). Both transcription factors (TFs) regulate gene expression during Cu deficiency through binding to Cu deficiency-responsive elements (5′-GTAC-3′) in promoters of their targets (Sommer et al., 2010; Yamasaki et al., 2009; Quinn et al., 2000; Birkenbihl et al., 2005; Garcia-Molina et al., 2014; Kropat et al., 2005). Recent transcriptome analyses revealed that SPL7 is required for the expression of the iron (Fe)/Cu reductase oxidases, *FRO4* and *FRO5*, and several Cu transporters, including members of the copper transporter family, *COPT1* and *COPT2*, that together constitute the high-affinity Cu uptake system (Bernal et al., 2012; Gayomba et al., 2013; Jung et al., 2012; Yamasaki et al., 2009; Jain et al., 2014). Among other SPL7-regulated genes are COPT6, members of the yellow stripe-like transporter family, *YSL2* and *YSL3*, and the Cu chaperone *CCH*, which together contribute to Cu transport to photosynthetic tissues and Cu remobilization from sources to sinks upon senescence (Bernal et al., 2012; Gayomba et al., 2013; Jung et al., 2012; Yamasaki et al., 2009; Chu et al., 2010; Himelblau et al., 1998; Mira et al., 2001; Himelblau and Amasino, 2001). The SPL7-dependent Cu economy/metal switch mechanism involves the increased expression of Cu-responsive miRNAs that, in turn, facilitate mRNA degradation of abundant Cu-containing proteins such as Cu/Zn-superoxide dismutase (SOD), *CSD1*, *CSD2*, *plantacyanin* (*ARPN*), and *laccase-like multicopper oxidases* (*LAC2*, *LAC3*, *LAC4*, *LAC7*, *LAC12*, *LAC13*, and *LAC17*) (Abdel-Ghany and Pilon, 2008; Pilon, 2017; McCaig et al., 2005; Ravet et al., 2011; Shahbaz et al., 2015). CSD1 and CSD2 functions are replaced by the Fe-containing SOD, FSD1 (Burkhead et al., 2009). Because of the important role of SPL7 in Cu homeostasis, *spl7* mutants accumulate less Cu and develop slower unless Cu is added to the growth medium (Bernal et al., 2012; Yamasaki et al., 2009; Gayomba et al., 2013).

Despite the recognized role of Cu in plant fertility, our knowledge of the underlying molecular determinants that link Cu to reproduction is surprisingly limited. From what is known, genes encoding Cu transporters *COPT1*, *COPT2*, *COPT3*, and *COPT6* are expressed in pollen grains of Arabidopsis (Sancenón et al., 2004; Gayomba et al., 2013; Jung et al., 2012; Bock et al., 2006). *AtCOPT3* is expressed early in pollen development, while *AtCOPT1* is expressed at later stages (Bock et al., 2006). *AtCOPT1* antisense plants exhibit pollen abnormalities under Cu limited conditions and these defects can be rescued by Cu supplementation (Sancenón et al., 2004). *YSL3* is expressed in anthers and acts in concert with *YSL1* to ensure Arabidopsis fertility (Chu et al., 2010; Waters et al., 2006). In addition to Cu transporters, plantacyanins, which are classified as blue Cu proteins, have a conserved Cu binding site and are involved in pollen germination and pollen tube guidance (Rydén and Hunt, 1993; Einsle et al., 2000). Finally, Arabidopsis cytochrome *c* oxidase biogenesis factor 17 is expressed in anthers and roots (Attallah et al., 2007). These data suggest that Cu must function in anthers of Arabidopsis; however, the localization of Cu in plant reproductive structures has not been determined experimentally.

In addition to being controlled by Cu availability and other environmental factors (Endo et al., 2009; Smith and Zhao, 2016; Broadley et al., 2012), plant reproduction, including male fertility, is regulated by hormonal cues (Yuan and Zhang, 2015; Cheng et al., 2004; Cecchetti et al., 2008; Song et al., 2013). In this regard, jasmonic acid (JA) and related jasmonate metabolites, collectively called jasmonates, are lipid-derived signaling compounds that in addition to their well established role in plant responses to biotic and abiotic stresses, regulate stamen development and male fertility (Browse, 2009).

JA derives from fatty acids and its biosynthesis involves the sequential action of a series of enzymes (reviewed in Yuan and Zhang, 2015; Kombrink, 2012; Wasternack and Hause, 2013; Fonseca et al., 2009a; Schilmiller et al., 2007). Briefly, JA biosynthetic enzymes include fatty acid desaturases and phospholipases (PLA1/DAD1) that produce the JA precursor, α-linolenic acid. α-Linolenic acid is then converted to *cis*-(+)-12-oxophytodienoic acid in a series of sequential reactions catalyzed by the lipoxygenases, allene oxide synthase (AOS), allene oxide cyclases (AOC), and 12-*oxo*-phytodienoic acid reductase (OPR) (Supplemental Figure 1). JA can be further enzymatically modified into different derivatives including methyl jasmonate, *cis*-jasmone, jasmonyl-1-aminocyclopropane-1 carboxylic acid, and/or conjugated with amino acids such as isoleucine (Fonseca et al., 2009b), alanine, valine, or methionine (Yan et al.. 2016). The JA-isoleucine conjugate is a bioactive form of the hormone that binds to the JA receptor, COI1 (Fonseca et al.. 2009b; Sheard et al.. 2010). Mutants with defects in JA biosynthesis and/or signaling are male sterile, and this defect can be corrected by exogenous JA application (Caldelari et al., 2011; Ishiguro et al., 2001; McConn and Browse, 1996; Staswick et al., 2002; Feys et al., 1994; Park et al., 2002; von Malek et al., 2002; Stintzi and Browse, 2000). JA-dependent fertility defects are manifested by the decreased viability of pollen grains, delayed anther dehiscence, and the reduced length of stamen filaments (Caldelari et al., 2011; Ishiguro et al., 2001; McConn and Browse, 1996; Staswick et al., 2002). It has been recently shown that genes involved in JA biosynthesis are upregulated, and the endogenous concentration of JA is increased in the early stages of Fe deficiency in rice roots. Also, JA acts both positively and negatively on the expression of typical Fe deficiency-inducible genes depending on the plant Fe nutritional status (Kobayashi et al., 2016). The relationship between Cu deficiency and jasmonates has not yet been addressed.

Here, we show that a previously uncharacterized member of the basic helix-loop-helix (bHLH) family of transcription factors, CITF1 (Cu-DEFICIENCY INDUCED TRANSCRIPTION FACTOR1), acts with SPL7 in a complex integrated pathway that is required for Cu delivery to anthers and pollen fertility. We also found that Cu deficiency upregulates the expression of several JA biosynthetic genes in flowers and increases endogenous JA accumulation in leaves and that these effects are controlled in part by CITF1 and SPL7. Finally, we show that the JA-deficient mutant of Arabidopsis, lacking CITF1- and SPL7-regulated genes, *LOX3* and *LOX4*, is sensitive to Cu deficiency. Together, our data show that CITF1 and SPL7 regulate Cu homeostasis and JA biosynthesis.

RESULTS

Cu Deficiency Significantly Alters the Arabidopsis Flower Transcriptome

To initiate research on the role of Cu in plant fertility and to identify novel TFs regulating Cu homeostasis at the reproductive stage, we analyzed the response of the Arabidopsis flower transcriptome to Cu deficiency using RNA-seq. To determine the effect of Cu deficiency on the transcriptome during flower maturation, we collected flowers as flower buds: a mix of developmental stages 9-12 as defined by Sanders et al. (1999), Alvarez-Buylla et al. (2010), and Scott et al. (2004) and flowers at developmental stages 13-14 as defined by Sanders et al. (1999), Alvarez-Buylla et al. (2010), and Scott et al. (2004). The physiological status of plants was confirmed by analyzing Cu concentration in flowers of plants grown under Cu-sufficient or Cu-deficient conditions. Inductively coupled plasma mass spectrometry (ICP-MS) analysis revealed that the concentration of Cu in flowers of plants grown under Cu-sufficient conditions was 8.85 μg/g dry weight and dropped to 1.53 μg/g dry weight in flowers of plants grown under Cu deficiency. These internal Cu concentrations are within the expected range for Cu sufficiency and deficiency, respectively (Broadley et al. 2012).

We then employed Illumina sequencing for a genome-wide comparison of mRNA abundance in flowers of Cu-deficient versus Cu-sufficient wild-type (Col-0) plants. We obtained 58 and 56 million clean reads from mature flowers and flower buds, respectively (Supplemental Data Set 1). Of these, 87 and 90% reads from mature flowers and flower buds, respectively, were mapped to the Arabidopsis genome and employed for the estimation of transcript abundance and differential expression.

We found that 548 and 612 genes were differentially expressed in response to Cu deficiency in young and mature flowers, respectively (Figure 1A; Supplemental Data Sets 2 and 3). We then analyzed whether Cu deficiency altered the transcript abundance of genes implicated in Cu acquisition and transport as would be expected based on past studies in Arabidopsis (Bernal et al., 2012). In particular, we evaluated the expression of the Cu deficiency responsive genes encoding Cu transporters, *COPT1*, *COPT2*, *COPT6*, and *YSL2*, a member of the ZRT/IRT-like proteins, *ZIP2*, as well as ferric reductase oxidases *FRO3*, *FRO4*, and *FRO5* and the Cu chaperone *CCH* (Bernal et al., 2012; Yamasaki et al., 2009). We found that the expression of *COPT1*, *COPT2*, *COPT6*, *YSL2*, *YSL3*, and *CCH* was upregulated, while *ZIP2* was unchanged in flowers of Cu-deficient plants compared with flowers of plants grown under control conditions (Supplemental Data Sets 4 and 5). The transcriptional response to Cu deficiency was dynamic with regard to the developmental stage of flowers. For example, *COPT2* was upregulated 9.8-fold by Cu deficiency in young flowers but was not altered by Cu deficiency in mature flowers. The latter finding is consistent with the observation of Gayomba et al. (2013) showing the constitutive expression of *COPT2* in anthers and pollen grains in stage 14 flowers of Arabidopsis. By contrast, the expression of *YSL2* increased in response to Cu deficiency from 2.5-fold in young flowers to 4.9-fold in mature flowers, suggesting its increasingly important role during flower maturation. The expression of *COPT1*, *COPT6*, and *YSL3* was somewhat (1.7- to 1.8-fold) upregulated in young and mature flowers under Cu deficiency.

Concerning ferric reductase oxidase genes, the expression of *FRO3*, *4*, and *5* was not altered by Cu deficiency in flower buds or mature flowers. However, transcript levels of other FRO family members, *FRO2*, *FRO7*, and *FRO6*, were somewhat upregulated in flower buds (by 1.9-, 1.7-, and 1.6-fold, respectively). The expression of *FRO2* in response to Cu deficiency was unchanged in mature flowers, while the expression of *FRO6* and *FRO7* was upregulated by 2.1- and 2.2-fold, respectively (Supplemental Data Set 3). Perhaps *FRO6* and/or *FRO7* are involved in Cu(II) to Cu(I) reduction in reproductive organs.

We also evaluated the expression of Cu enzymes contributing to Cu quota (Burkhead et al., 2009; Bernal et al., 2012) and found that both flower buds and mature flowers exhibited Cu deficiency responses indicative of the prioritization of Cu reserves (Supplemental Data Sets 2 and 3). These changes in flowers were manifested by the reduction of *CSD1* and *CSD2* transcripts and the upregulation of *FSD1*. In addition, the transcript levels of genes encoding other enzymes recognized as contributing to Cu quota were significantly decreased in flower buds, mature flowers, or both (Supplemental Table 1). The transcriptional response of flowers to Cu deficiency was validated by RT-qPCR (Supplemental Figure 2). Taken together, our RNA-seq data revealed the substantial reorganization of the flower transcriptome in response to Cu deficiency.

The Expression of an Uncharacterized bHLH Family Member, *CITF1*, Is Highly Upregulated in Flowers of Arabidopsis in Response to Cu Deficiency

The global functional analysis of RNA-seq data using MetGenMap revealed enrichment in transcripts encoding TFs among differentially expressed genes. Specifically, 19.2% and 15.5% of Arabidopsis TF genes were upregulated by Cu deficiency by more than 2-fold in young and mature flowers, respectively (Supplemental Data Sets 6 and 7) and the expression of 26 TF transcripts was upregulated in both flower buds and mature flowers (Figure 1B). Only two TF transcripts were downregulated in both flower buds and mature flowers (Figure 1B). Among upregulated TFs, the expression of a previously uncharacterized TF from the basic helix-loop-helix family, *bHLH160*, was upregulated by 23.6- and 147.7-fold in young and mature flowers, respectively (Supplemental Data Sets 6 and 7). This pattern of *bHLH160* expression was confirmed by RT-qPCR (Figure 1C), and we designated this gene as *CITF1*. We then tested whether Fe deficiency would alter the transcript abundance of *CITF1* because it has been shown that Cu deficiency might cause secondary Fe deficiency symptoms (Bernal et al., 2012), and mRNA expression of *COPT2* is also upregulated by Fe deficiency in roots of Arabidopsis (Colangelo and Guerinot, 2004). However, unlike *COPT2*, the expression of *CITF1* was downregulated by Fe deficiency (Figure 1D), indicating that *CITF1* is highly responsive to Cu status in plants and is a novel regulator of Cu homeostasis.

CITF1 Localizes to the Nucleus in Arabidopsis Protoplasts

To examine the subcellular localization of CITF1, it was fused at the C terminus to EGFP in the SAT6-EGFP-N1-Gate vector and transiently expressed in Arabidopsis protoplasts under the control of the constitutive cauliflower mosaic virus CaMV 35S promoter

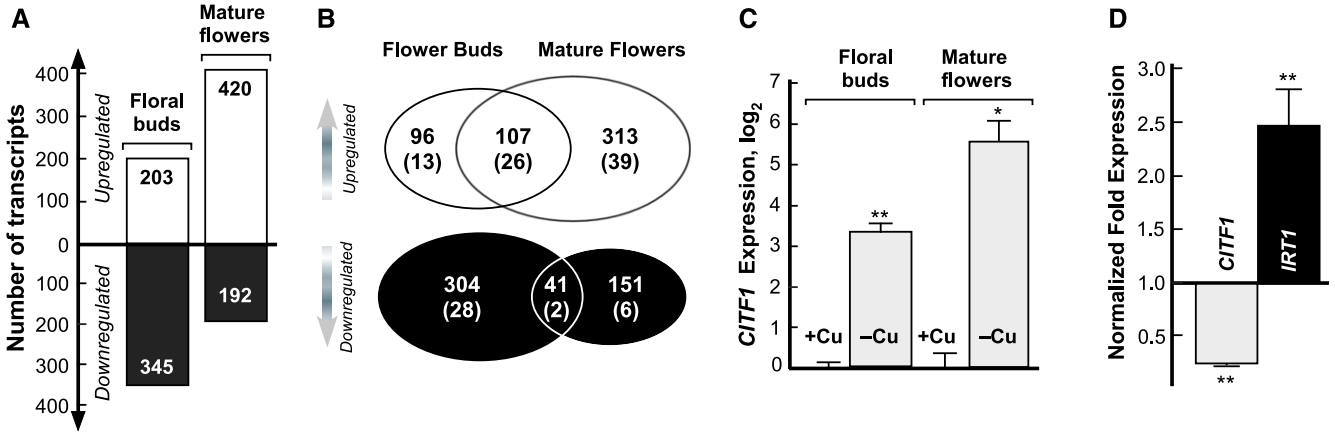

Figure 1. Cu Deficiency Significantly Alters the Flower Transcriptome in Arabidopsis.

(A) Number of Cu deficiency-responsive genes in flower buds and mature flowers, according to RNA-seq. White bars represent the number of upregulated genes (ratio ≥ 2, FDR < 0.05). Black bars represent the number of downregulated genes (ratio ≤ 0.5, FDR < 0.05).

(B) Venn diagrams that were generated by R program VennDiagram-package (version 1.6.17) (Chen and Boutros, 2011) show the number of common and unique Cu-responsive genes in flower buds and mature flowers. White and black ovals represent up- and downregulated genes, respectively. Overlaps show the number of genes regulated in both tissues. Cu-responsive TFs are shown in parenthesis.

(C) RT-qPCR analysis of *CITF1* transcript abundance in floral buds and mature flowers under Cu limitation. Results are presented relative to the expression of *CITF1* in the wild type grown under Cu-sufficient conditions. Error bars indicate SE ($n = 3$ independent experiments with flowers collected from 4 plants per experiment). Asterisks (*P < 0.05; **P < 0.001) indicate statistically significant differences of the mean values.

(D) RT-qPCR analysis of *CITF1* transcript abundance in roots of 10-d-old seedlings of wild-type Arabidopsis grown on 0.5× MS solid medium without or with 200 μM of the Fe chelator BPS. The expression of the Fe transporter-encoding gene, *IRT1*, was used as a control to verify Fe-deficient conditions. Results are presented relative to the expression of each gene in plants grown on 0.5× MS agar media without BPS and are designated as 1. Error bars indicate SE (n = 3 replicate plates with roots collected from ~20 seedlings/plate). Asterisks indicate statistically significant differences of the mean values between control and treated plants (P < 0.001, based on REST; Pfaffl et al., 2002).

(Figure 2A; Supplemental Figure 3A). Protoplasts were also transfected with the empty SAT6-EGFP-N1 vector (Supplemental Figure 3B). EGFP-mediated fluorescence was present in the nucleus of CITF1-EGFP-transfected protoplasts and did not overlap with chlorophyll autofluorescence (Figure 2A). To ascertain the nuclear localization of CITF1-EGFP, the transfected protoplasts were costained with a DNA-specific fluorescent probe, DAPI (4′,6-diamidino-2-phenylindole) (Kapuscinski, 1995). After short-term incubation, DAPI stained the nucleus, and DAPI-mediated fluorescence overlapped with CITF1-EGFP-mediated fluorescence but not with chlorophyll-mediated fluorescence (Figure 2A; Supplemental Figure 3A). EGFP was present as a soluble protein in the cytosol, and its fluorescence did not overlap with chlorophyll autofluorescence in protoplasts transfected with the empty vector (Supplemental Figure 3B). Based on these results, we concluded that CITF1 localizes to the nucleus in Arabidopsis protoplasts, which is consistent with its predicted function as a transcriptional regulator.

CITF1 Is Essential for the Normal Growth of Arabidopsis under Cu-Limited Conditions

To study the role of *CITF1* in Cu homeostasis, two *citf1* T-DNA insertion alleles, designated as *citf1*-1 and *citf1*-2, were obtained from the ABRC (Alonso et al., 2003). In *citf1*-1 and *citf1*-2, T-DNA was inserted in the 1st exon and 3′-untranslated region of *CITF1*, respectively, leading to a loss of the *CITF1* transcript in the *citf1*-1 allele and a significant depletion of the *CITF1* transcript in the *citf1*-2 allele (Supplemental Figures 4A to 4C). We also generated the *citf1*-1 allele expressing the genomic *CITF1* fragment (*CITF1*$_{pro}$:*CITF1*) for functional complementation analysis. We found that both *citf1*-1 and *citf1*-2 plants were more sensitive to Cu deficiency than the wild type as indicated by their smaller stature (Figure 2B; Supplemental Figure 4D), the appearance of chlorotic spots on mature leaves (Figure 2C; Supplemental Figure 4E), and fewer seeds in siliques (Figure 2D). The genomic *CITF1* fragment complemented Cu deficiency phenotypes of *citf1*-1 (Figure 2B). These results indicate that the increased sensitivity of the *citf1* mutant to Cu deficiency is due to a lesion in *CITF1*. Given the similarity of phenotypes in both alleles, and because *citf1*-2 is a leaky allele, we used *citf1*-1 (from here on *citf1*) in subsequent studies.

Copper Accumulation Is Altered in Tissues of the *citf1*-1 Mutant

We next tested whether Cu uptake into roots and/or delivery to shoots is altered in the *citf1* mutant. To do so, we compared Cu concentrations in roots, leaves, and flowers in the hydroponically grown *citf1* mutant versus the same tissues in the wild type, both grown under Cu replete or deficient conditions. We collected mature leaves (source leaves) and young leaves (sinks) separately because different transport mechanisms for most mineral nutrients occur in source and sink leaves (Broadley et al., 2012). We found that the concentration of Cu in all tested tissues of the *citf1* mutant was significantly lower compared with wild-type plants,

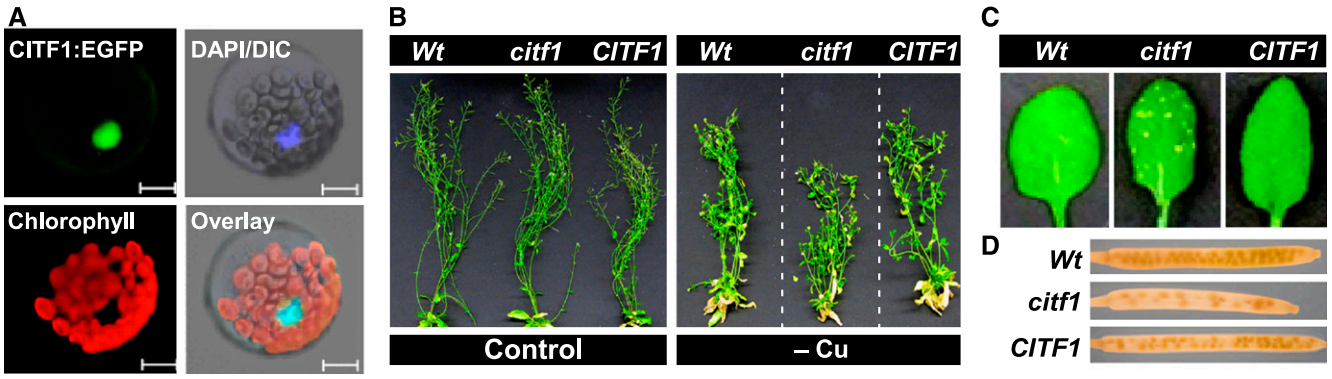

Figure 2. *CITF1* Is Essential for the Normal Growth of Arabidopsis under Cu-Limited Conditions.

(A) CITF1-EGFP localizes to the nucleus in Arabidopsis protoplasts. A superimposed image (Overlay) shows that CITF1-EGFP colocalizes with DAPI fluorescence but not with chlorophyll-mediated autofluorescence. Bar = 10 μm.
(B) The wild type, the *citf1*-1 mutant, and the *citf1*-1 mutant expressing the genomic *CITF1* fragment were grown hydroponically with or without 0.125 μM $CuSO_4$.
(C) and **(D)** Representative images of the 4th bottommost leaf and silique, respectively, collected from plants grown under Cu deficiency.
(B) to **(D)** Representative results from three independent experiments. In each experiment, at least 10 plants per line per condition were analyzed.

when plants were grown under Cu sufficient conditions (Figure 3A). Nevertheless, the *citf1* mutant grew normally because the level of Cu was sufficient to sustain the normal growth of mutant plants (Broadley et al., 2012). We also found that Cu uptake into roots and delivery to mature leaves and flowers was most affected, while Cu movement to young leaves was the least affected (Figure 3A). Specifically, we found that roots, mature leaves, and flowers of the *citf1* mutant contained 38, 21, and 26% less Cu, respectively, than corresponding tissues of wild-type plants (Figure 3A). By contrast, young leaves of the *citf1* mutant contained only 9% less Cu than young leaves of the wild-type plants (Figure 3A).

Copper concentrations were significantly reduced in all tissues and all plant lines grown under Cu-deficient conditions (Figure 3A). We did not find statistically significant differences in Cu accumulation in roots and young leaves of Cu deficient *citf1* versus wild-type plants (Figure 3A). However, we found that mature leaves of the *citf1* mutant accumulated 24% more Cu, while flowers accumulated 36% less Cu than corresponding tissues of the wild type, suggesting a defect in Cu remobilization during deficiency. Collectively, we interpreted our results to suggest that CITF1 is involved in the high-affinity uptake of Cu into the root, as well as Cu remobilization for delivery to reproductive organs.

The Transcriptional Response of *COPT2*, *FRO4*, and *FRO5* to Cu Deficiency Is Altered in the *citf1* Mutant

We next tested whether the increased sensitivity of the *citf1* mutant to Cu deficiency and decreased Cu accumulation in its tissues is associated with altered expression of genes encoding the high-affinity COPT/FRO Cu uptake system in the root. We found that CITF1 regulates *FRO4* and *FRO5* expression in roots of plants even under control growth conditions (Figure 3B). The transcript abundance of *COPT2* in *citf1* roots was similar to that of roots in wild-type plants grown under control conditions. As expected, Cu deficiency increased the transcript abundance of *COPT2*, *FRO4*, and *FRO5* in wild-type plants (Figure 3B; Bernal et al., 2012). This effect of Cu deficiency was partially abolished in the *citf1* mutant (Figure 3B).

CITF1 and *SPL7* Act in a Complex Integrated Pathway Regulating Cu Homeostasis

To examine the relationship between *CITF1* and the master regulator of Cu homeostasis, *SPL7*, we generated the *citf1*-1 *spl7*-1 double mutant (from here on *citf1 spl7*). We then compared the growth and development of the *citf1 spl7* double mutant with each of the single mutants as well as wild-type plants grown in soil and fertilized with the N-P-K fertilizer and standard hydroponic medium containing 0.125 μM $CuSO_4$. We found that the growth of the *citf1 spl7* double mutant was arrested in the early seedling stage, and the double mutant eventually died (Figure 4A), unlike the wild-type and *citf1* mutant plants that grew well under the same conditions. The *spl7* mutant was somewhat smaller than the wild type (Figure 4A), which is consistent with the observations of Yamasaki et al. (2009). The synthetic lethality for the two independent loci, *citf1* and *spl7*, suggested that *CITF1* and *SPL7* act in an integrated pathway and that the regulation of Cu homeostasis in Arabidopsis is more complex than was previously thought.

We then tested whether the transcriptional response of *CITF1* to Cu deficiency depends on SPL7. We found that *CITF1* expression was higher in roots and flowers than in leaves under control conditions (Figure 4B) and that the Cu deficiency response of *CITF1* in leaves entirely depended on SPL7 (Figure 4B). By contrast, *CITF1* expression in roots and flowers was still upregulated in the *spl7* mutant under Cu deficiency (Figure 4B). We concluded that other TFs in addition to SPL7 regulate the transcriptional response of *CITF1* to Cu deficiency in roots and flowers. These results are also consistent with our suggestion that *CITF1* and *SPL7* act in the complex integrated pathway regulating Cu homeostasis.

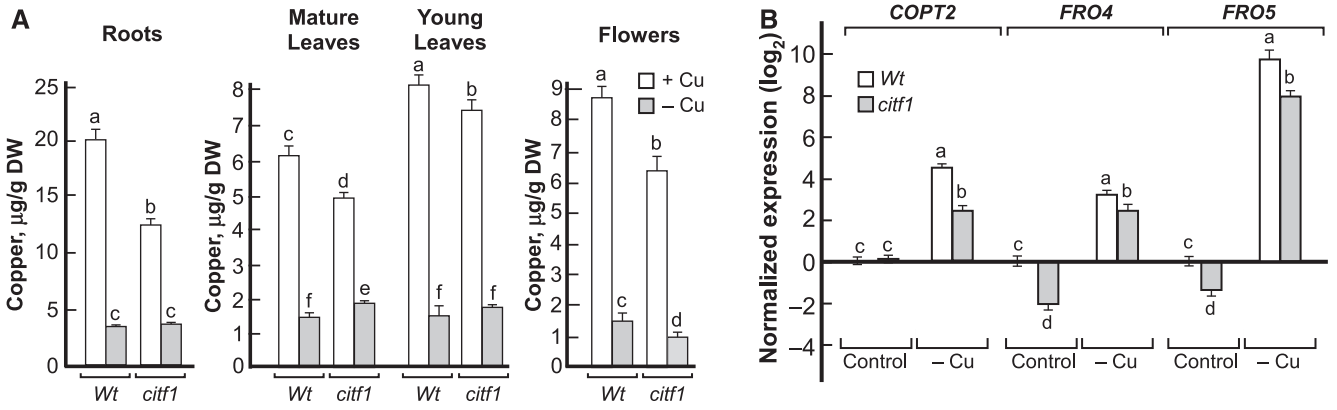

Figure 3. CITF1 Regulates Cu Uptake and Delivery to Reproductive Organs.

(A) The concentration of Cu in roots, mature and young leaves, and mix stage flowers of the wild type and the *citf1* mutant. For the analysis of Cu concentrations in root and leaf tissues, plants were grown with or without 0.125 μM $CuSO_4$ (white and gray bars, respectively) for 4 weeks. For the analysis of Cu concentrations in flowers, plants were grown with 0.5 μM $CuSO_4$ for 8 weeks (white bars). Cu deficiency in flowers was achieved by withholding Cu for the last 3 weeks of growth (gray bars). Shown values are arithmetic means ± SD ($n = 5$ independent experiments; tissues from 4 plants were pooled together in each independent experiment). Different letters indicate statistically significant differences between means ($P < 0.05$, based on ANOVA).

(B) The transcript abundance of *COPT2*, *FRO4*, and *FRO5* in roots of the wild type (open bars) and the *citf1* mutant (gray bars). Plants were grown hydroponically with 0.125 μM $CuSO_4$ (Control) for 5 weeks. A subset of plants was grown without Cu for the last 2 weeks (– Cu). Values are arithmetic means ± SE ($n = 3$ independent experiments; tissues from 4 plants were pooled together in each independent experiment). Different letters indicate statistically significant differences in gene expression under control and Cu deficient conditions ($P < 0.05$, based on REST; Pfaffl et al., 2002).

Cu Supplementation Rescues the Seedling Lethal Phenotype of the *citf1 spl7* Plants

To test whether Cu could rescue the seedling lethality of the *citf1 spl7* double mutant, wild-type, *citf1* and *spl7* single, and *citf1 spl7* double mutants were grown in soil fertilized with 5 or 50 μM $CuSO_4$. The growth of the wild type and the *citf1* mutant was indistinguishable under both conditions (Figure 4C). Although the *citf1* mutant accumulated less Cu in the shoot compared with the wild type, it was sufficient to support its growth and development (Figure 4D). The *spl7* mutant also developed into a fertile adult under 5 μM of Cu, but it was smaller than the wild type and the Cu concentration in its shoots was significantly lower, being within the deficiency range (Figures 4C and 4D). Fertilization with 50 μM $CuSO_4$ fully rescued the growth and Cu accumulation defect of the *spl7* mutant (Figures 4C and 4D). Concerning the *citf1 spl7* double mutant, 5 μM $CuSO_4$ rescued its seedling lethality, but its growth was arrested at the early reproductive stage (Figure 4C). Consistent with this phenotype, Cu concentration in shoots of the double mutant was extremely low and was just at the detection level of the ICP-MS (Figures 4C and 4D). At a higher concentration of Cu (50 μM), the *citf1 spl7* double mutant was also able to grow to the reproductive stage but was still smaller than the other plant lines even though its shoot Cu concentration was 6.6 ± 1.4 μg/gDW, which is regarded sufficient to sustain growth and development (Figures 4C and 4D).

The *citf1 spl7* Double Mutant Has Altered Flower Development, Morphology, Pollen Fertility, and Anther Dehiscence

Although the *citf1 spl7* double mutant was able to reach the reproductive stage under high Cu supplementation, it did so with a significant delay compared with the wild type and each of the single mutants. It also had 54% fewer flowers, shorter inflorescences with atypical internode spacing, shorter siliques, and almost no seeds compared with wild-type, *citf1*, and *spl7* single mutants (Figures 5A, 5B, and 5D; Supplemental Figure 5A). We also noticed that the *citf1 spl7* double mutant had significantly longer pistils than filaments (Figure 5C; Supplemental Figure 5B) that would restrict self-pollination and could be the reason for the significantly decreased fertility.

The reciprocal cross-pollination between the *citf1 spl7* mutant and the wild type revealed that wild-type pollen fertilized the *citf1 spl7* plants, suggesting that the female fertility of the double mutant was normal (Figure 5E). By contrast, the pollen from the double mutant failed to fertilize wild-type or the *citf1 spl7* pistils (Figures 5F and 5G). These results suggested that male, but not female, fertility was compromised in the double mutant. Consistently, the number of pollen grains per anther was 90% lower and the viability of the pollen was reduced in the double mutant compared with the wild type and each of the single mutant lines (Figures 6A to 6C).

We also analyzed anther dehiscence, as the resulting pollen dispersal is an important component of the successful reproduction process. We found that anther dehiscence was delayed in *citf1*, *spl7*, and the *citf1 spl7* mutants at stage 13 of flower development (at anthesis; Sanders et al., 1999; Alvarez-Buylla et al., 2010; Scott et al., 2004)) compared with the wild type (Figure 6D). Anther dehiscence was still delayed in stage 14 flowers of the *citf1 spl7* double mutant, unlike the wild type and each of the single mutants, in which 100% of anthers were dehisced (Figure 6D).

CITF1 and SPL7 Are Required for Cu Delivery to Flowers

We next analyzed the spatial distribution of Cu in flowers using synchrotron-based x-ray fluorescence (SXRF) microscopy. This

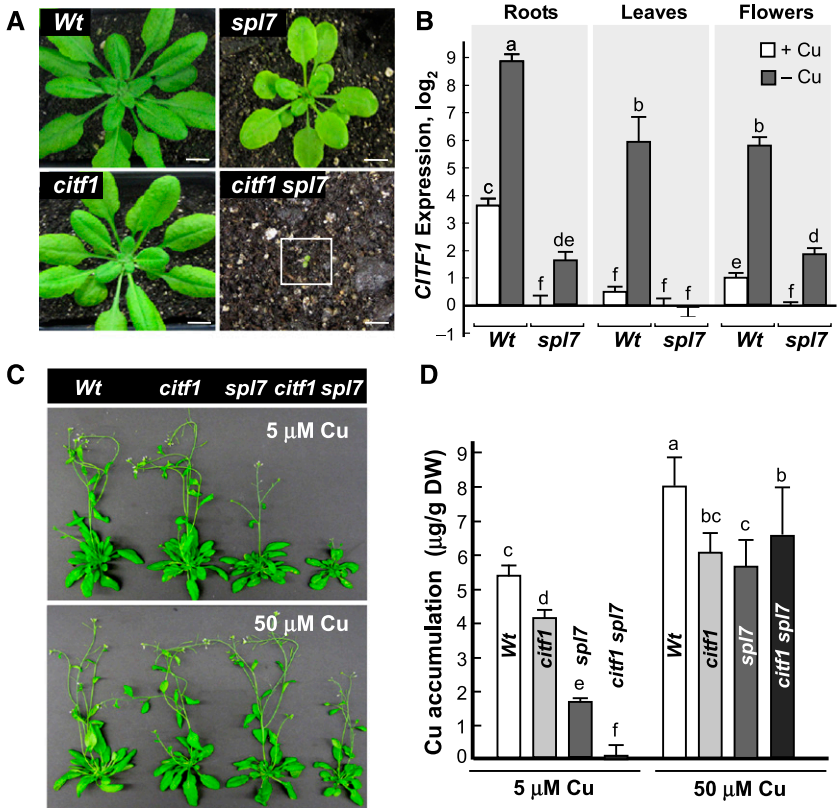

Figure 4. CITF1 and SPL7 Act in a Complex Cu Regulatory Pathway.

(A) Seeds of the indicated plant lines were germinated and grown in soil, and fertilized with the N-P-K fertilizer and a standard nutrient solution (Zhai et al., 2014). Note the retarded growth of the *citf1 spl7* double mutant seedling (inside a white square) that eventually died.

(B) RT-qPCR comparison of *CITF1* transcript abundance in tissues of wild-type and *spl7* mutant plants, grown hydroponically with (open bars) or without 0.25 μM $CuSO_4$ (gray bars) as specified in Methods. Error bars indicate SE ($n = 3$ independent experiments; tissues from 4 plants were pooled together in each independent experiment). Different lowercase letters indicate statistically significant differences of the mean values ($P < 0.05$, based on REST; Pfaffl et al., 2002).

(C) Different plant lines were germinated hydroponically, transferred to soil, and fertilized every 2 weeks with a standard N-P-K fertilizer containing the indicated concentrations of Cu. Data are from one plant per line representative of 10 plants per line analyzed.

(D) Concentration of Cu in shoots of different plant lines grown as described in **(C)**. Error bars indicate SE ($n = 5$ independent experiments; tissues from 4 plants were pooled together in each independent experiment). Different lowercase letters indicate statistically significant differences of the mean values ($P < 0.05$, based on ANOVA).

method is superior to other high precision element imaging techniques because it allows the visualization of essential cellular metals with high sensitivity and high spatial resolution in situ, reducing the artifacts of sample preparation (Donner et al., 2012). SXRF microscopy revealed that the bulk of Cu in flowers of wild-type plants was in anthers and carpels (Figure 7A; Supplemental Figure 6). Analysis of the different mutant lines disclosed that, compared with wild-type flowers, Cu accumulation was somewhat lower in anthers and carpels of the *citf1* mutant, and was further reduced in anthers and carpels of the *spl7* mutant (Figure 7A; Supplemental Figure 6). By contrast, Cu was barely detectable in the majority of the *citf1 spl7* anthers (Figure 7A; Supplemental Figure 6). We note that some flowers of the double mutant accumulated low but detectible concentrations of Cu in anthers (Supplemental Figure 6 and the last flower on the right in Figure 7A). This result is consistent with the ability of a subset of flowers in the double mutant to produce some seed.

We also compared the distribution of Fe in these genotypes since SPL7 mediates crosstalk between Fe and Cu homeostasis (Bernal et al., 2012). We found that similar to Cu, the bulk of Fe was associated with anthers in wild-type plants (Figure 7B). Unlike Cu, however, Fe accumulation in anthers did not change significantly in *spl7* and *citf1* single or *citf1 spl7* double mutants (Figure 7B). These data show that SPL7 and CITF1 act in the complex integrated pathway regulating the delivery of Cu to anthers and carpels.

Cu Deficiency, CITF1, and SPL7 Regulate the Expression of Genes from the JA Biosynthetic Pathway

The sterility phenotypes described above resemble some of the phenotypes of JA-related mutants (Browse, 2009). Analysis of our RNA-seq data revealed that the expression of several genes from

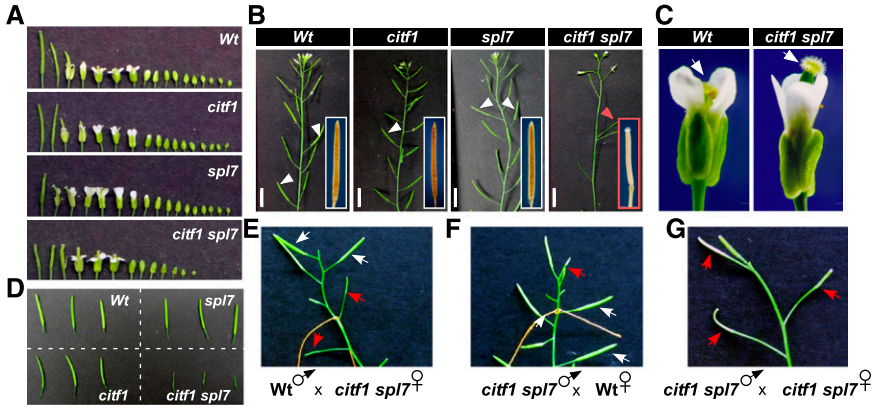

Figure 5. The *citf1 spl7* Double Mutant Has a Defect in Male Fertility.

(A) Flowers that were collected from the main inflorescence in the indicated plant lines are shown from the oldest (left) to the youngest (right).
(B) Primary inflorescences of different plant lines. White arrowheads and insets show siliques filled with seeds in wild-type, *citf1*, and *spl7* plants, and a red arrowhead and inset show unfertilized pistils in the *citf1 spl7* double mutant. Bar = 10 mm.
(C) Altered flower morphology of the *citf1 spl7* double mutant compared with the wild type. White arrows indicate pistils.
(D) Example of siliques collected from the bottom (left) to the top (right) of the main inflorescence of different plant lines.
(E) to **(G)** Results from reciprocal hand-pollination between the wild type and the *citf1 spl7* double mutant. White arrows indicate siliques filled with seeds in the *citf1 spl7* double mutant after pollination with wild-type pollen **(E)** or self-pollination in the wild type **(F)**. Red arrows indicate unfertilized pistils in the *citf1 spl7* mutant resulting from self-pollination **(E)**, pollination of wild-type pistils with the *citf1 spl7* pollen **(F)**, or the manually pollinated *citf1 spl7* mutant **(G)**. In **(A)** to **(G),** plant lines were germinated hydroponically, transferred to soil, and fertilized weekly with a standard N-P-K fertilizer containing 10 μM $CuSO_4$. Data are from one plant per line representative of 10 plants per line analyzed.

the JA biosynthetic pathway, *LOX3*, *LOX4*, *AOS*, *AOC3*, *OPR3*, *KAT5*, and *JAR1*, were upregulated by Cu deficiency in flower buds and/or mature flowers (Supplemental Table 2 and Supplemental Figure 1). It should be noted that the relationship between the JA metabolic pathway and Cu homeostasis has not yet been established. We therefore tested whether the upregulation of JA biosynthetic genes in flowers under Cu deficiency was SPL7 and/or CITF1-dependent.

RT-qPCR analysis revealed that the expression of *LOX3*, *LOX4*, *AOS*, and *OPR3* was, in part, dependent on CITF1 and SPL7 even in flowers of plants grown under control conditions (Figure 8A). Furthermore, the upregulation of the expression of these genes as well as *KAT5* and *JAR1* by Cu deficiency depended on CITF1 and/or SPL7 (Figure 8A). We also found that while the JA biosynthetic genes *DAD1*, *AOC1*, and *AOC2* did not respond transcriptionally to Cu deficiency, their expression in young and/or mature flowers of plants grown under control conditions was under the control of both CITF1 and SPL7 (Figure 8B). The *citf1 spl7* double mutant requires significant Cu supplementation and has a significant delay in developing to the reproductive stage; therefore, we did not

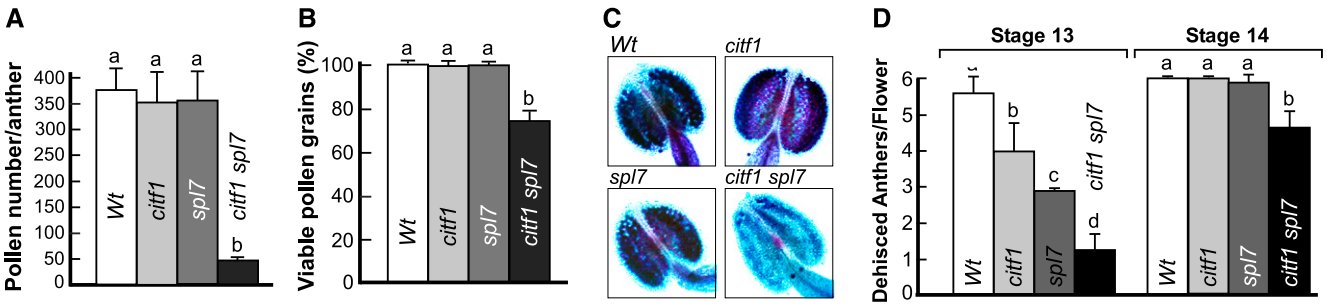

Figure 6. CITF1 and SPL7 Are Required for Pollen Fertility.

(A) Total pollen production per anther of stage 13 flowers in the indicated plant lines (Sanders et al., 1999; Alvarez-Buylla et al., 2010; Scott et al., 2004).
(B) Percentage of viable pollen in the indicated plant lines. In **(A)** and **(B)**, different plant lines were germinated hydroponically, transferred to soil, and fertilized biweekly with a standard N-P-K fertilizer supplemented with 50 μM $CuSO_4$.
(C) Alexander staining of pollen grains in anthers from the indicated plant lines. Viable pollen grains were stained dark and light violet, while nonviable pollen grains were pale turquoise. Note that most pollen was aborted in the *citf1 spl7* double mutant.
(D) Number of dehisced anthers per flower. In **(A)** to **(D)**, $n = 10$ flowers with 6 anthers/flower analyzed per plant line. Different letters indicate statistically significant differences of mean values ($P < 0.05$, based on ANOVA).

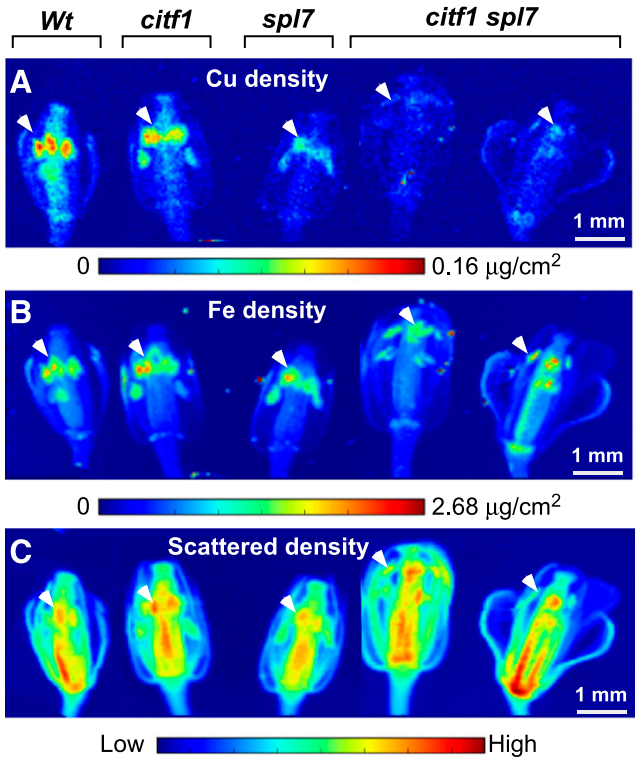

Figure 7. CITF1 and SPL7 Are Required for Cu Delivery to Anthers.

(A) and **(B)** SXRF analysis of Cu **(A)** and Fe **(B)** localization in flowers of the wild type and indicated Arabidopsis mutants. Seeds were germinated hydroponically. Three-week-old seedlings were transferred to soil and fertilized every week with the standard N-P-K fertilizer supplemented with 10 μM $CuSO_4$. Flowers at stage 13 of flower development were collected and the spatial distribution of Cu was analyzed by SXRF. The 2D Cu and Fe raster maps were acquired at 40-μm resolution and 0.25 s/pixel dwell time. X-ray fluorescence was captured using a Vortex ME-4 silicon drift detector. White arrows point to anthers.
(C) Total fluorescence density to visualize flower organs.

use it for the analysis of the expression of JA biosynthetic genes in reproductive tissues. Based on these results, we concluded that CITF1 and SPL7 regulate the expression of genes from the JA biosynthetic pathway.

The SPL7-CITF1 Pathway Is Involved in JA Biosynthesis

We next measured JA concentrations in different plant lines. JA is synthesized mainly in leaves, but is also produced in stamens of flowers at stages 11-12 of flower development (Ishiguro et al., 2001; Scott et al., 2004). Given that it was impractical to collect sufficient amounts of stamens as well as flowers from the double mutant for measurable JA analysis, we analyzed leaves of different plant lines grown under control or Cu-deficient conditions. The concentration of JA in the majority of samples from the *spl7* and *citf1 spl7* double mutant was at the detection limit when we used the standard JA extraction procedures (Supplemental Figure 7A). Therefore, to reach conclusive results, we scaled up our JA analysis sample preparation method as described in Methods, which enabled us to quantify JA concentration in the leaves of all mutant lines. These studies yielded the following findings: First, Cu deficiency significantly increased JA concentrations in the leaves of wild-type plants (Figure 9A). Second, the induction of JA synthesis by Cu deficiency was impaired in the *citf1* mutant (Figure 9A). Third, JA concentrations were 82% lower in the *spl7* mutant versus the wild type under both control and Cu-deficient conditions (Figure 9A). This result uncovered a novel aspect of SPL7 function: In addition to Cu homeostasis, SPL7 may regulate JA biosynthesis. Finally, JA concentrations in leaves of the *citf1 spl7* double and *spl7* single mutants were similar, regardless of whether plants were grown under control or Cu-deficient conditions (Figure 9A). These data are consistent with JA concentration trends in different mutant lines obtained using standard extraction procedures (Supplemental Figure 7A). Based on these data, we concluded that the SPL7-CITF1 integrated pathway is involved in JA synthesis in leaves. In this pathway, SPL7 plays a predominant role under both Cu-sufficient and -deficient conditions.

Exogenous JA Does Not Rescue the Fertility Defect of the *citf1 spl7* Double Mutant

Some of the fertility defects of the *citf1 spl7* double mutant such as decreased pollen viability and delayed anther dehiscence (Figures 6B to 6E) resemble phenotypes of male infertile mutants from the JA biosynthesis and/or signaling pathways (Ishiguro et al., 2001; Sanders et al., 1999; McConn and Browse, 1996; Feys et al., 1994). Therefore, we tested whether exogenous JA application could rescue the fertility defect of the *citf1 spl7* double mutant as it does for some male infertile JA biosynthesis mutants. In addition to the *citf1 spl7* plants, we used the male sterile *lox3 lox4* double mutant lacking two lipoxygenases, LOX3 and LOX4, that are essential for JA synthesis (Supplemental Figure 6; Caldelari et al. 2011) and the expression of their genes is regulated by CITF1 and SPL7 (Figure 8A). Consistent with previous findings (Caldelari et al., 2011), the male sterility of this mutant was rescued by the exogenous application of JA to flower buds (Supplemental Figure 7B). By contrast, JA application did not rescue the fertility defect of the *citf1 spl7* double mutant (Supplemental Figure 7B). We were also not able to rescue fertility of the *citf1 spl7* double mutant by applying a combination of JA and Cu.

The JA Synthesis Mutant, *lox3 lox4*, Is Sensitive to Cu Deficiency

Although we were not able to rescue the fertility defects of the *citf1 spl7* double mutant with JA, the increased JA accumulation in leaves of Cu-deficient Arabidopsis (Figure 9A) and decreased JA accumulation in Cu deficiency-sensitive *citf1* and *spl7* mutants (Figures 2B to 2D and 9A) prompted us to test whether JA is needed for the normal growth of plants under Cu deficiency. To address this question, we used the *lox3 lox4* double mutant. We found that the *lox3 lox4* double mutant was highly sensitive to Cu deficiency as evidenced by the appearance of extensive chlorotic spots on mature and middle age leaves (Figures 9B and 9C), which resembled the phenotype of the *citf1* mutant under low Cu (Figures 2C and 9C). These data suggest that JA and/or α-linolenic acid derivatives, the downstream products of LOX3 and LOX4 action

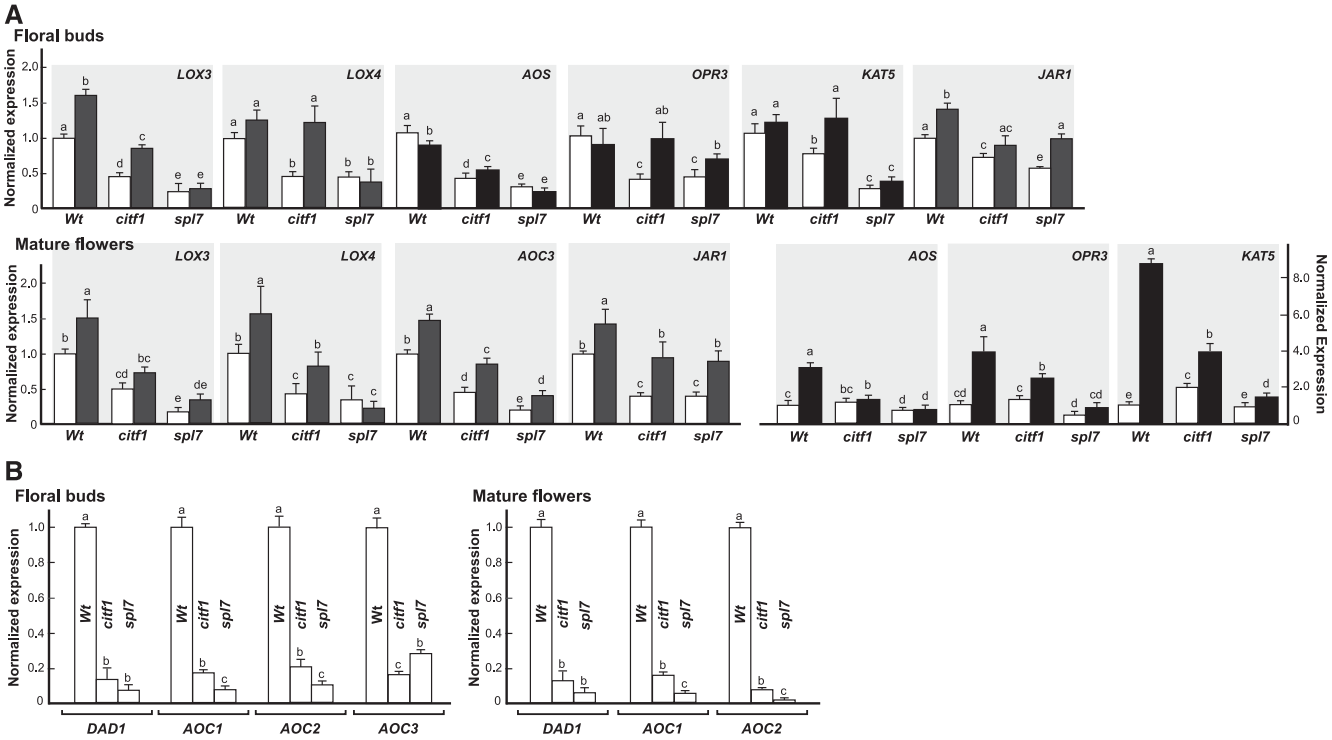

Figure 8. SPL7 and CITF1 Regulate the Expression of JA Biosynthetic Genes.

(A) The expression of JA biosynthetic genes in floral buds or mature flowers is upregulated by Cu deficiency and this response depends on SPL7 and/or CITF1. Indicated plant lines were grown hydroponically with 0.5 μM $CuSO_4$ for 7 weeks (white bars); a subset of plants was grown without Cu for the last week to achieve Cu deficiency (black bars).

(B) The expression of JA biosynthetic genes in flowers of wild-type, *citf1*, and *spl7* mutant plants. Plants were grown hydroponically with 0.5 μM $CuSO_4$ for 7 weeks prior to analysis. Values are arithmetic means ± SE of $n = 3$ technical replicates of 3 independent experiments. Flower tissues were pooled from four plants per independent experiment. Results are presented relative to the expression of each gene in the wild type that was designated as 1. Different lowercase letters indicate statistically significant differences of the mean values ($P < 0.05$, based on REST; Pfaffl et al., 2002).

(Supplemental Figure 1), are important for the normal growth of plants under Cu deficiency.

JA Regulates the Expression of *CITF1*

We then investigated whether JA could alter the expression of Cu-responsive genes. In silico analysis using the electronic fluorescent pictograph (eFP) browser (Winter et al., 2007) revealed that exogenously applied JA downregulated the expression of *CSD1*, *CSD2*, *UCC2*, and to a lesser degree *ARPN* in roots and shoots of Arabidopsis seedlings (Supplemental Figure 8). Products of these genes contribute to cellular Cu quota (Supplemental Table 1; Bernal et al., 2012) and Cu economy under Cu deficiency (Burkhead et al., 2009). With regard to Cu deficiency-responsive Cu transporters, *YSL2* expression was significantly upregulated and *ZIP2* expression somewhat upregulated in both roots and shoots after JA treatment (Supplemental Figure 8). *YSL2* was also among the transporter genes whose expression was most highly upregulated by Cu deficiency in flower buds and mature flowers (Supplemental Data Set 1). The expression of the high-affinity Cu transporters *COPT1* and *COPT2* was not affected by JA (Supplemental Figure 8). Likewise, the expression of SPL7 was not altered by JA (Supplemental Figure 8). Data on *CITF1* were not included in the eFP browser. Therefore, we tested the effect of JA treatment on *CITF1* expression using RT-qPCR. We found that JA treatment significantly increased the transcript abundance of *CITF1* in roots and this transcriptional response depended only partially on SPL7 (Figure 9D).

DISCUSSION

The global demand for high-yielding crops is increasing due to continuing population growth, a trend that is forcing the utilization of mineral nutrient-deficient marginal lands for agricultural purposes. In this regard, plant deficiency for the essential micronutrient Cu occurs in alkaline soils that occupy ~30% of the world's arable land and in organic soils (Shorrocks and Alloway, 1988; Broadley et al., 2012). It has been known for decades that in addition to causing stunted growth and chlorosis of leaves, Cu deficiency reduces plant fertility and seed/grain set (Shorrocks and Alloway, 1988; Garcia-Molina et al., 2014; Sancenón et al., 2004; Broadley et al., 2012; Burkhead et al., 2009). However, our knowledge of the underlying molecular determinants that link Cu nutrition with plant reproduction and transcriptional regulatory

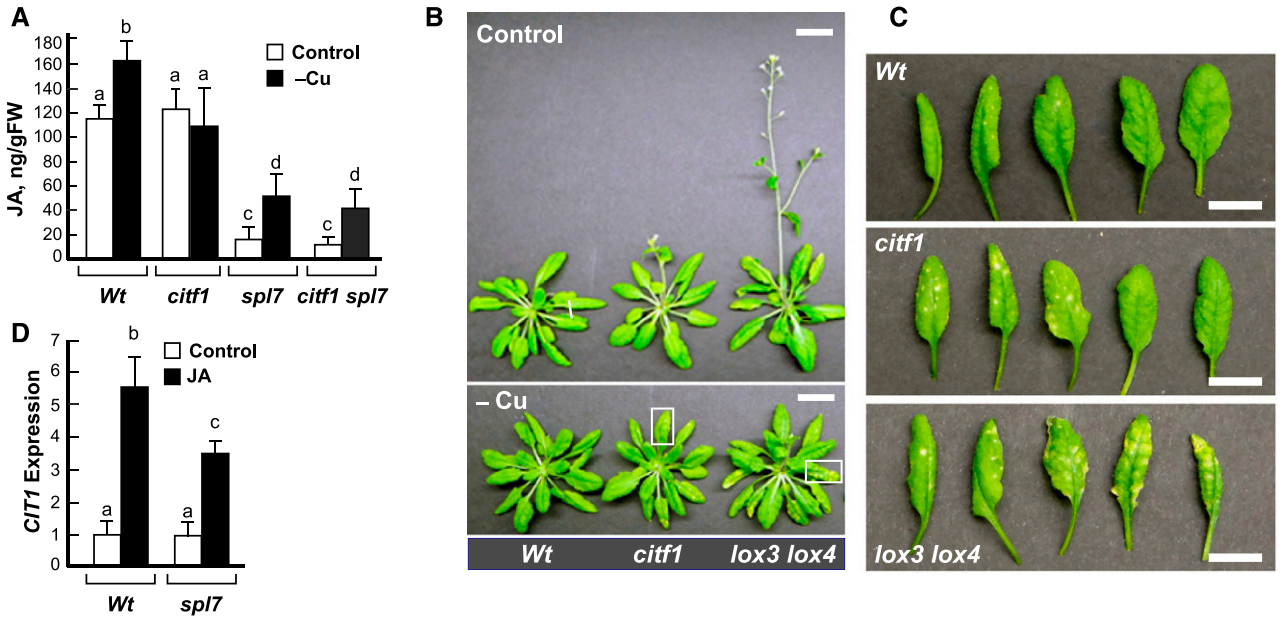

Figure 9. CITF1 and SPL7 Are Involved in JA Synthesis.

(A) The concentration of JA in leaves of 5-week-old plants, grown hydroponically with 0.5 μM $CuSO_4$ for the entire time (Control) or without Cu for the last 2 weeks (− Cu). Lowercase letters are used to indicate statistically significant differences between genotypes and conditions ($P < 0.05$). Error bars indicate SE ($n = 3$ independent experiments).

(B) Indicated plant lines were germinated and grown hydroponically for 40 d with (Control) or without 0.125 μM $CuSO_4$ (− Cu). The figure shows representative plants from 12 plants per line and per condition analyzed. The *lox3 lox4* mutant flowered earlier than other plant lines. The white box encloses an example of a Cu deficiency-affected leaf. Bar = 2 cm.

(C) Leaves were collected from plant lines grown under Cu deficiency as described in **(B)**. Leaves were ordered from old on the left to young on the right. Note the increased chlorosis in leaves from *citf1* and *lox3 lox4* mutants compared with the wild type. Bar = 1 cm.

(D) RT-qPCR analysis of transcript abundance of *CITF1* in roots of 23-d-old plants after short-term (24 h) treatment with 10 μM JA. Lowercase letters indicate statistically significant differences between genotypes and conditions ($P < 0.05$, based on REST; Pfaffl et al., 2002). Error bars indicate SE ($n = 3$ technical replicate of $n = 3$ independent experiments with 4 plants used to pool root tissues per each experiment).

networks that orchestrate the response to Cu deficiency is surprisingly limited. Thus far, SPL7, an Arabidopsis homolog of the algal Cu sensor, CRR1, is the only TF with an established function in Cu homeostasis in vascular plants (Yamasaki et al., 2009; Garcia-Molina et al., 2014; Bernal et al., 2012; Kropat et al., 2005).

Analysis of the response of the Arabidopsis flower transcriptome to Cu deficiency has led us to the discovery of a highly Cu deficiency-responsive TF that we designated as CITF1 (Figure 1C; Supplemental Data Sets 6 and 7). CITF1 (alias bHLH160) belongs to the bHLH family and is essential for the normal growth of Arabidopsis under Cu deficiency (Figures 2B to 2D; Supplemental Figure 4). Because the *citf1*-1 mutant also accumulated less Cu in roots, shoots, and flowers (Figure 3A), we concluded that CITF1 is involved in the regulation of Cu uptake into roots as well as internal Cu transport. Consistent with this suggestion, CITF1 regulated the expression of *FRO4* and *FRO5* even under Cu replete conditions and was, in part, responsible for the increased expression of these two genes as well as *COPT2* under Cu deficiency (Figure 3B). Furthermore, we found that Cu uptake and delivery to mature leaves as well as flowers was most affected, while Cu movement to young leaves was the least affected Cu transport process in the *citf1* mutant (Figure 3A). Additionally, we found that mature leaves of Cu-deficient *citf1* plants accumulated more Cu, while flowers accumulated less Cu than corresponding tissues of Cu-deficient wild type (Figure 3A). It is noteworthy that the transport of minerals to sinks (e.g., roots, young leaves, and reproductive organs) occurs mainly via the phloem-based remobilization from sources such as mature leaves during the vegetative stage or from senescing tissues during the reproductive stage (Broadley et al., 2012; Himelblau and Amasino, 2001). Therefore, a more pronounced effect of *CITF1* loss of function on Cu delivery to flowers during the reproductive stage than to young leaves during the vegetative stage suggests that CITF1 might regulate Cu remobilization to reproductive organs during senescence in addition to its involvement in high-affinity Cu transport.

In silico analysis of past microarray and RNA-seq studies of Cu deficiency-regulated genes in seedlings and vegetative tissues of Arabidopsis identified *CITF1* among SPL7-regulated genes (Bernal et al., 2012; Yamasaki et al., 2009). However, our studies suggested that the relationship between CITF1 and SPL7 is more complex than was previously thought (Figure 10). First, we found that unlike *citf1* and *spl7* single mutants, the *citf1 spl7* double mutant was not able to grow in soil under Cu-sufficient conditions (Figure 4A). Second, while the transcriptional Cu deficiency response of *CITF1* in leaves entirely depended on SPL7 (Figure 4B), *CITF1* expression in roots and flowers was still upregulated in the *spl7* mutant under Cu deficiency (Figure 4B). Third, while Cu

treatment allowed the *citf1 spl7* double mutant to progress to the reproductive stage, it remained largely infertile with only several siliques per plant filled with seeds (Figure 5B). Reciprocal hand-pollination between the *citf1 spl7* double mutant and the wild type showed that the male fertility of the double mutant was severely compromised (Figures 5E to 5G). We then found that the *citf1 spl7* double mutant produced 90% less pollen than the wild type or each single mutant line. Furthermore, ~20% of the pollen produced by the *citf1 spl7* double mutant was unviable (Figures 6A to 6C). The anther dehiscence of the *citf1 spl7* double mutant was delayed as well (Figure 6D). Based on these results, we concluded that other TFs in addition to SPL7 regulate the transcriptional response of *CITF1* to Cu deficiency in roots and flowers (Figure 10) and that the loss of *CITF1* and *SPL7* function in the *citf1 spl7* double mutant severely inhibits plant reproduction via reducing pollen fertility, pollen dispersal, and flower development.

The dramatic loss of fertility in the *citf1 spl7* double mutant could be interpreted to mean that CITF1 and SPL7 coregulate the delivery of Cu to specific floral structures, e.g., anthers, the sites of pollen development. To test this hypothesis, we compared the spatial distribution of Cu in floral organs of the wild type, *citf1* and *spl7* single, and *citf1 spl7* double mutants using SXRF microscopy. We found that the bulk of Cu localizes to anthers in flowers and that SPL7 and CITF1 are both required for Cu delivery to these reproductive structures (Figure 7A). It is noteworthy that although the role of Cu in plant fertility has been recognized for many decades, its spatial distribution in floral organs was unknown. Finding the high concentration of Cu in anthers and carpels that are directly involved in reproduction underscores the importance of Cu in flower fertility. We further show that Cu accumulation was somewhat lower in anthers and carpels of the *citf1* mutant, was further reduced in anthers and carpels of the *spl7* mutant, and was barely detectable in the majority of the *citf1 spl7* anthers (Figure 7A; Supplemental Figure 6). In contrast to Cu, Fe accumulation in anthers was similar in all plant lines (Figure 7B). Together, these results highlight the significance of both CITF1 and SPL7 in Cu delivery to anthers and plant reproduction. Future work will discriminate whether the majority of Cu in anthers is associated with the anther wall or pollen grains, or both, as well as the precise role of Cu in pollen development.

In addition to previously identified Cu deficiency-regulated transporter genes, *COPT1*, *COPT2*, *COPT5*, and *YSL3* in vegetative tissues (Bernal et al., 2012; Yamasaki et al., 2009), the expression of 33 and 39 transporter genes is upregulated by Cu deficiency in flower buds and mature flowers, respectively (Supplemental Data Sets 4 and 5). Which of these transporter genes are involved in Cu transport and are under CITF1 and/or SPL7 transcriptional control is yet to be determined. We note that the concentration of Cu in pistils of the *citf1 spl7* double mutant was significantly decreased (Figure 7A; Supplemental Figure 6). The role of Cu in pistils has yet to be determined as well. Collectively, these data show that CITF1 and SPL7 act in the complex integrated pathway to ensure Cu delivery to reproductive organs (Figure 10).

Detailed analysis of the RNA-seq data revealed that the expression of several genes from the JA biosynthetic pathway was upregulated by Cu deficiency in floral buds and mature flowers (Supplemental Table 2). Therefore, we tested whether the

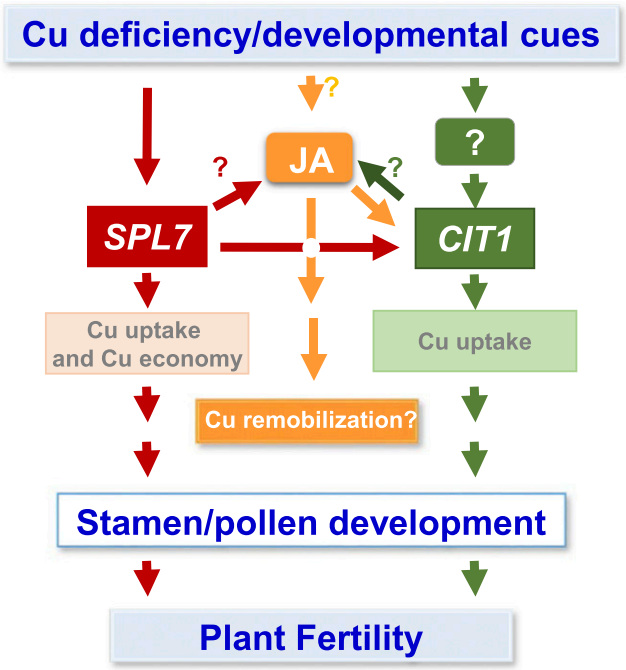

Figure 10. The CITF1- and SPL7-Dependent Integration of Cu Homeostasis and JA Synthesis.

Copper deficiency resulting either from limited Cu availability in the environment or from the increasing demands of the developing shoot upregulates the expression of *CITF1* via SPL7 as well as via other yet unidentified TFs. Cu deficiency, SPL7, and CITF1 regulate the expression of JA biosynthesis genes, and SPL7 is essential for the JA synthesis. *CITF1* expression and JA biosynthesis are regulated by a positive feedback loop: JA increases *CITF1* expression, while *CITF1* regulates the expression of JA biosynthesis genes. SPL7 also regulates the expression of genes involved in Cu uptake and internal Cu economy, while CITF1 regulates the expression of genes involved in Cu uptake. Whether CITF1 also controls the expression of genes involved in Cu economy, which transcription factors, in addition to SPL7, regulate *CITF1* expression under Cu deficiency, and how Cu deficiency, SPL7, and CIT1 are involved in JA metabolic pathway are unknown (indicated by question marks).

expression of genes from the JA biosynthetic pathway and JA accumulation depends on CITF1 and/or SPL7. We found that Cu deficiency increased the transcript abundance of several JA biosynthetic genes in a CITF1- and SPL7-dependent manner, including *LOX3*, *LOX4*, *AOS*, *AOC3*, *OPR3*, *KAT5*, and *JAR1* in flower buds and/or mature flowers, and also stimulated JA synthesis in leaves (Figures 8A and 9A; Supplemental Figure 7A). We also found that that the expression of *DAD1*, *AOC1*, and *AOC2* was under CITF1 and SPL7 control under Cu-sufficient conditions (Figure 8B). Based on levels of JA accumulation in different mutant backgrounds (Figure 9A), we concluded that SPL7 has a more dominant role on JA biosynthesis compared with CITF1. Whether changes in the expression of JA biosynthesis genes are an indirect consequence of Cu deficiency and/or alteration in gene expression in *citf1* and *spl7* mutants or whether JA biosynthesis genes are direct CITF1 or SPL7 targets still needs to be determined.

It is noteworthy that reduced pollen viability and delayed anther dehiscence in the *citf1 spl7* double mutant (Figures 6B to 6E) resemble some of the phenotypes of JA biosynthesis and/or signaling mutants (Ishiguro et al., 2001; Sanders et al., 1999; McConn and Browse, 1996; Feys et al., 1994; Park et al., 2002). Therefore, we hypothesized that there is a relationship between Cu deficiency-stimulated expression of JA biosynthetic genes, CITF1 and SPL7, and fertility. However, we were not able to rescue the fertility defect of the *citf1 spl7* double mutant by exogenous JA application (Supplemental Figure 7B). We concluded that the compromised fertility of the *citf1 spl7* double mutant is likely not associated with the decreased JA synthesis in its leaves and could be related to the inability of the mutant to deliver Cu to specific sites within anthers. This conclusion is further supported by the finding that the internal concentration of JA in leaves of the *spl7* single mutant was as low as in the *citf1 spl7* double mutant under both control and Cu-deficient conditions (Figure 9A). However, unlike the *citf1 spl7* double mutant that was infertile under control conditions, the *spl7* mutant was fertile and accumulated Cu in anthers, albeit at a lower level than the wild type (Figures 5A and 7A).

Recently, reduced pollen viability under Cu deficiency was found in the Arabidopsis double mutant lacking SPL7 and its interacting partner, KIN17 (immunological kinship to RecA protein 17; Angulo et al., 1991; Garcia-Molina et al., 2014). Interestingly, the *kin17-1 spl7-2* double mutant, similar to the *citf1 spl7* double mutant, has altered flower morphology when grown under Cu-deficient conditions (Garcia-Molina et al., 2014). Whether JA accumulation in leaves and Cu delivery to anthers as well as pollen fertility are altered in the *kin17 spl7* double mutant under these conditions is unknown.

Although we were not able to rescue the fertility defect of the *citf1 spl7* double mutant with the exogenous application of JA, the observed relationship between Cu deficiency-stimulated, and CITF1- and SPL7-regulated JA synthesis (Figures 8 and 9A) was intriguing and prompted us to test whether JA plays a role in plant growth under Cu deficient conditions. If it does, then JA-deficient mutants would be more sensitive to Cu deficiency than wild-type plants. To test this prediction, we used the JA-deficient *lox3 lox4* double mutant lacking the CITF1- and SPL7-regulated genes, *LOX3* and *LOX4*. We found that the *lox3 lox4* double mutant was highly sensitive to Cu deficiency (Figures 9B and 9C). This finding and the increased expression of JA biosynthetic genes and JA accumulation in leaves of wild-type plants (Figures 8A and 9A) suggest that some oxylipins and/or JA play a role in Cu homeostasis.

The newly established link between SPL7 and CITF1-mediated Cu homeostasis, fertility, and JA metabolism is intriguing. While SPL7 is required for the expression of JA biosynthetic genes under control conditions, and both SPL7 and CITF1 are required for JA synthesis under Cu deficiency, JA itself regulates a limited number of Cu-responsive genes. None of the genes encoding the high-affinity Cu uptake system seem to be upregulated by JA (Supplemental Figure 8), suggesting that JA might not stimulate Cu uptake into roots. However, among the JA-upregulated genes were *CITF1* (Figure 9D) and *YSL2* (Supplemental Figure 8). The latter gene is implicated in lateral movement of transition metals and their delivery to sinks (e.g., flowers) (DiDonato et al., 2004). In addition, the expression of several genes contributing to Cu economy and, thus, downregulated under Cu deficiency (Burkhead et al., 2009) was also downregulated by JA treatment (Supplemental Figure 8). Interestingly, the concentration of JA increases in senescing leaves in Arabidopsis, and the expression of JA biosynthesis genes such as *LOX3*, *LOX4*, *AOC1*, *AOC2*, *AOC3*, and *OPR3* is upregulated (He et al., 2002). These genes are also regulated by CITF1 and SPL7 (Figure 8). Because during leaf senescence mineral nutrients are recycled to other plant organs with developing flowers and seeds representing major sinks (Himelblau and Amasino, 2001), and because our data suggest that CITF1 regulates Cu remobilization to reproductive organs (Figure 3A), we hypothesize that CITF1 and SPL7 function in leaves via JA to regulate Cu remobilization processes to ensure successful fertility. However, this suggestion still needs to be tested experimentally.

To conclude, we propose that CITF1 and SPL7 act in a complex integrated pathway to ensure Cu uptake and delivery to reproductive organs (Figure 10). Both SPL7 and CITF1 regulate the expression of several JA biosynthetic genes under Cu sufficient conditions as well as under Cu deficiency. Whether SPL7 and CITF1 regulate the expression of JA biosynthesis genes directly needs to be determined experimentally. *CITF1* expression and JA biosynthesis are regulated by a positive feedback loop: exogenous application of JA increases *CITF1* expression, while the expression of JA biosynthetic genes is decreased in the *citf1* mutant. Whether the increased JA production is needed to stimulate Cu remobilization from leaves to developing reproductive organs to ensure pollen development is yet to be determined. Future work will also establish the mechanism of CITF1 function in Cu homeostasis, the precise sites of Cu action in pollen development, transport systems responsible for Cu delivery to reproductive organs, and sites of interaction between Cu homeostasis and the jasmonate pathway.

METHODS

Plant Materials

All plant lines used in the study were in the *Arabidopsis thaliana* Columbia (Col-0) background. Seeds of the *SPL7* mutant (SALK_093849; *alias spl7*-1) mutant were obtained from Toshiharu Shikanai (Kyoto University, Japan). Seeds of the *lox3 lox4* double mutant were a generous gift of Edward Farmer (University of Lausanne, Switzerland). These mutants were previously described (Caldelari et al., 2011; Yamasaki et al., 2009). Two *CITF1* mutant alleles, SALK_073160 (*alias citf1*-1) and SAIL_711_B07 (*alias citf1*-2), were obtained from the ABRC (Alonso et al., 2003). Homozygous mutants bearing T-DNA insertions were selected by PCR using genomic DNA as a template and the LBb1.3 for the SALK line and RP or LB1 for the SAIL line and RP primer pairs indicated in Supplemental Table 3. To generate a double *citf1 spl7* mutant, the *citf1*-1 allele was crossed into the *spl7*-1 mutant, and the homozygous double mutant (*citf1 spl7*) was selected by PCR using the genomic DNA as the template and the LBb1.3 and RP primer pairs for *CITF1* and *SPL7* genes indicated in Supplemental Table 3.

Growth Conditions and Experimental Treatments

Different Arabidopsis plant lines were grown either on solid 0.5× Murashige and Skoog (MS) medium (pH 5.7) (Murashige and Skoog, 1962) or hydroponically (Zhai et al., 2014). For growing plants on solid medium, seeds were surface-sterilized as described (Zhai et al., 2014). Seeds of

uniform size were sown on solid 0.5× MS medium supplemented with 1% (w/v) sucrose, 0.7% (w/v) agar (Sigma-Aldrich; A1296) and the indicated concentrations of the Fe chelator bathopenanthrolinedisulfonic acid (BPS) (Rapisarda et al., 2002). After stratification at 4°C for 2 d in darkness, seeds were germinated and grown vertically for 10 d in a growth chamber at 22°C, 14-h-light/10-h-dark photoperiod at a photon flux density of 110 μmol m^{-2} s^{-1}.

For growing plants hydroponically, seeds were surface-sterilized and sown in 10 μL pipette tips containing 0.7% (w/v) agar. The tip of pipette tips was cut prior to placing them into floats made of foam boards. This experimental setup allowed roots to immerse into the hydroponic solution, which was replaced every week (Zhai et al., 2014). The standard solution contained 0.125 μM $CuSO_4$ (Zhai et al., 2014). To study the effect of JA on the expression of *CITF1*, 3-week-old plants were transferred to fresh hydroponic medium and treated with or without 10 μM JA for 24 h. In experiments involving the *spl7-1* mutant, all plant lines were grown in the presence of 0.25 μM $CuSO_4$. In experiments involving the *citf1 spl7* double mutant, all plant lines were grown hydroponically from seed in a medium containing 0.5 μM $CuSO_4$. For achieving Cu deficiency in roots and shoots, plants were grown hydroponically for 5 weeks in total; Cu was omitted from the medium from a subset of plants in the last 2 weeks.

For growing the *citf1 spl7* double mutant and corresponding single mutants and wild type in soil, all plant lines were initially germinated and grown hydroponically with 0.5 μM $CuSO_4$. After 4 weeks (12-leaf stage), plants were transferred to soil (Lambert 111) for subsequent development to the reproductive stage. Plants were fertilized with the standard N-P-K fertilizer supplemented with the indicated concentrations of $CuSO_4$. In all cases, plants were grown at 22°C, 14-h-light/10-h-dark photoperiod a photosynthetic photon flux density of 110 μmol m^{-2} s^{-1} produced with cool-white fluorescent bulbs supplemented by incandescent lighting.

High-Throughput Sequencing of mRNA, Sequence Mapping, and Differential Gene Expression Analysis

Arabidopsis wild-type plants were grown hydroponically for 7 weeks under Cu-sufficient (0.25 μM $CuSO_4$) conditions. To achieve Cu deficiency, a subset of plants was grown without Cu in the last week. Flowers were collected as flower buds (a mix of developmental stages 9-12 as defined; Sanders et al., 1999; Alvarez-Buylla et al., 2010; Scott et al., 2004) and as mature flowers at developmental stages 13-14 (Sanders et al., 1999; Alvarez-Buylla et al., 2010; Scott et al., 2004). Total RNA was isolated using TRIzol reagent (Invitrogen). Three micrograms of total RNA was used to construct the strand-specific RNA-seq libraries using procedures described (Zhong et al., 2011). Three replicates per condition were used in these experiments. RNA-seq libraries were sequenced on the Illumina HiSeq 2500 system using the single-end mode. The Illumina raw reads were processed using Trimmomatic (Bolger et al., 2014) to remove adaptor and low-quality sequences. Reads shorter than 40 bp were discarded. The resulting reads were aligned to the rRNA database (Quast et al., 2013) using Bowtie (Langmead et al., 2009) allowing three mismatches, and those aligned were discarded. The final clean reads were aligned to the Arabidopsis genome sequence (TAIR 10) using TopHat (Trapnell et al., 2009) allowing one mismatch. Following alignment, for each gene model, the count of mapped reads from each sample was derived and normalized to RPKM (reads per kilobase of exon model per million mapped reads). Differentially expressed genes were identified using edgeR (Robinson et al., 2010) with the raw count data. Raw P values were corrected for multiple testing using the false discovery rate (FDR; Benjamini and Hochberg, 1995). Genes with an FDR of less than 0.05 and fold changes of greater than or equal to 2 were regarded as differentially expressed genes.

Plant MetGenMap (http://bioinfo.bti.cornell.edu/cgi-bin/MetGenMAP/home.cgi), a web-based analysis and visualization package, was used to identify enriched GO terms from the gene expression data sets. The identification of overrepresented (enriched) GO terms was implemented based on the CPAN perl module (Boyle et al., 2004), which uses the hypergeometric distribution to calculate the significance of the GO term enrichment. The gene functional classification was analyzed based on their GO annotations. Arabidopsis transcription factors and transcriptional regulators were identified and classified using the iTAK program (Zheng et al., 2016). Arabidopsis transporter information was obtained from the plant transporter database (Tchieu et al., 2003).

Plasmid Construction and Plant Transformation

For functional complementation assays, a 2.9-kb *CITF1* genomic fragment spanning the entire *CITF1* locus was PCR-amplified from genomic DNA isolated from Arabidopsis roots. Primers were designed to include att*B* sites on the resultant PCR product (Supplemental Table 3). The DNA fragment was introduced into the *DONR222* entry vector (Invitrogen) before recombination with *RCS2-hpt* destination vector (Chung et al., 2005). The resulting construct was transformed into the *citf1*-1 mutant using the floral dip method (Clough and Bent, 1998). Several one-copy insertion homozygous lines were selected based on segregation ratios on the selection medium containing hygromycin.

To study the subcellular localization of CITF1 in Arabidopsis protoplasts, the full-length *CITF1* cDNA without a stop codon was amplified by RT-PCR from RNA isolated from roots of Arabidopsis grown under Cu-deficient conditions (Supplemental Table 3). The resultant cDNA was cloned by recombination into the *SAT6-N1-EGFP-Gate* vector (Jung et al., 2012) to create the CITF1-EGFP fusion and express it under the control of the CaMV 35S promoter.

Subcellular Localization and Fluorescence Microscopy

The $35S_{pro}$-*CITF1-EGFP* construct and *SAT6-N1-EGFP*, lacking the cDNA insert, were transfected individually into Arabidopsis protoplasts using previously established procedures (Zhai et al., 2009). To visualize nuclei, protoplasts were incubated at room temperature with 5 μL of DAPI·2HCl (10 mg/mL). After 15 min of incubation, protoplasts were pelleted by centrifugation at 100*g* for 2 min at room temperature, and supernatant was aspirated while protoplasts were resuspended in W5 solution prior to fluorescent microscopy. EGFP- and DAPI-mediated fluorescence and chlorophyll autofluorescence were visualized using FITC (for EGFP), DAPI, and rhodamine (for chlorophyll) filter sets of the Axio Imager M2 microscope equipped with the motorized Z-drive (Zeiss). Images were collected with the high-resolution AxioCam MR camera. Images were processed using the Adobe Photoshop software package, version 12.0.

RT-qPCR and Data Analysis

Root, shoot, and flower tissues were collected from plants grown as described above and were flash-frozen in liquid nitrogen before the homogenization using a mortar and a pestle. Samples were collected between 7 and 8 Zeitgeber time, where the Zeitgeber hour 1 is defined as the first hour of light after the dark period. Total RNA was isolated using TRIzol reagent (Invitrogen) according to the manufacturer's instructions. One microgram of total RNA was treated with DNase I (New England Biolabs) prior to the first-strand cDNA synthesis. The AffinityScript QPCR cDNA synthesis kit (Agilent Technologies) was used for producing cDNA for subsequent RT-qPCR analyses.

Prior to RT-qPCR analysis, primer and cDNA concentrations were optimized to reach the target and normalizing gene amplification efficiency of 100% ± 10%. Two microliters of 15-fold diluted cDNA was used as a template for RT-qPCR in a total volume of 15 μL containing a 500 nM concentration of each PCR primer, 50 mM KCl, 20 mM Tris-HCl, pH 8.4, 0.2 mM of each dNTP, and 1.25 units of iTaq DNA polymerase in iQ SYBR Green Supermix (Bio-Rad). PCR was performed using the CFX96 real-time PCR system (Bio-Rad). The thermal cycling parameters were as follows:

denaturation at 95°C for 3 min, followed by 39 cycles of 95°C for 10 s and 55°C for 30 s. Amplicon dissociation curves (i.e., melting curves) were recorded after cycle 39 by heating from 60°C to 95°C with 0.5°C increments and an average ramp speed of 3.3°C s^{-1}. Real-time PCR experiments were conducted using three independent experiments and three technical replicates, unless indicated otherwise. Data were normalized to the expression of *ACTIN 2*. The fold difference ($2^{-\Delta\Delta Ct}$) was calculated using the CFX Manager Software, version 1.5 (Bio-Rad).

Analysis of Cu Concentration

Plants were grown hydroponically in the standard solution (Zhai et al., 2014), with or without the indicated concentration of Cu. Roots, shoots, and flowers were harvested. Roots were desorbed by washing with 10 mM EDTA for 5 min followed by washing in a solution of 0.3 mM BPS and 5.7 mM sodium dithionite for 10 min before rinsing three times with deionized water. Elemental analysis was performed using ICP-MS as described (Zhai et al. 2014).

SXRF Microscopy

Wild-type, *citf1*, *spl7*, and *citf1 spl7* mutants were germinated and grown hydroponically prior to transfer into soil (Lambert 111). Once in soil, plants were fertilized every week with the standard N-P-K fertilizer supplemented with 10 μM $CuSO_4$. Flowers at stage 13 (as defined; Sanders et al., 1999; Alvarez-Buylla et al., 2010; Scott et al., 2004) were detached immediately prior to analysis, placed in the wet chamber made between two layers of metal-free Kapton film, and mounted onto 35-mm slide mounts. The spatial distribution of Cu and Fe in hydrated flower tissues was imaged via SXRF microscopy at the F3 station at the Cornell High Energy Synchrotron Source (CHESS). The 2D Cu and Fe raster maps were acquired at 40-μm resolution, 0.25 s/pixel dwell time using a focused, monochromatic incident x-ray beam at 12.2 keV and photon flux of $\sim 1 \times 10^{10}$ photons/s. The monochromatic beam was generated with 0.6% energy bandwidth multilayers. Focusing was achieved using a single-bounce moncapillary (named PEB605) fabricated at CHESS. These settings did not cause detectable damage to plant tissues within the 4- to 6-h scans required for analysis of the full set of genotypes. Element-specific x-ray fluorescence was detected using a Vortex ME-4 silicon drift detector. Quantifications were done by calibrating using thin metal foil film standard during each experiment and expressed as μg cm^{-2}. Data were processed with the software Praxes, which was developed at CHESS and employs PyMCA libraries in batch mode (Solé et al., 2007).

Pollen Viability and Anther Dehiscence Assays

Pollen viability was analyzed using Alexander staining (Alexander, 1969). Briefly, stage 12 floral buds were collected from the indicated plant lines and fixed overnight in ethanol and acetic acid (3:1 ratio). Anthers were then dissected on a slide and pollen was tapped out. A drop (~15 μL) of Alexander stain was added and a cover slip was sealed with rubber cement. Slides were incubated on a hot plate (65°C) for 1.5 h. Viable pollen grains were stained dark violet, while nonviable pollen grains were pale turquoise. The numbers of viable and aborted pollens were counted and images were collected using the Axio Imager M2 microscope (Zeiss). Anther dehiscence was analyzed by observing stage 13 and 14 flowers (Alvarez-Buylla et al., 2010) on main inflorescences using a Leica S6E stereomicroscope at 40× magnification. Ten flowers with six anthers/flower were analyzed per plant line.

LC-MS Analysis of JA

Leaf tissues were collected from 5-week-old plants grown hydroponically with 0.5 μM $CuSO_4$ for the entire time or without Cu for the last 2 weeks. Wild-type, *citf1*, and *spl7* single mutants and the *citf1 spl7* double mutant were grown in the same Magenta box for each treatment condition. Leaves from two plants per line and per condition were pooled for JA extraction. Collected tissues were flash-frozen in liquid N_2 prior to subsequent manipulations. Given that the internal JA concentration in tissues of plants grown under control conditions is low, we scaled up the JA extraction procedure described (Wang et al., 2007) to enable us to quantify and compare JA concentration in different mutant lines. Briefly, 400 to 500 mg of frozen tissues was ground to a fine powder using a mortar and a pestle. JA was extracted with 1 mL of the solvent containing isopropanol:H_2O:HCl at a ratio of 2:1:0.005. A hundred microliter liquate of D_5-JA (80 pg/μL) was added to each sample as an internal standard and samples were vortexed and centrifuged at 14,000 rpm, 4°C for 20 min in the Eppendorf centrifuge 5424. The supernatant was collected, mixed with 1 mL of dichloromethane, and centrifuged again for phase separation at 11,500 rpm, 4°C for 2 min. The aqueous top layer and the middle layer were discarded. The remaining solvent was air-dried in the fume hood. The dried residue was reconstituted in methanol and filtered through a 0.45-μm nylon filter for subsequent analyses by liquid chromatography-mass spectrometry (LC-MS) using the triple quadrupole LC-MS system (Quantum Access; Thermo Scientific) at the Cornell Chemical Ecology Core Facility. JA concentration was calculated by normalizing to the internal standard and was then converted to ng/g fresh weight. Given that some samples from the *spl7* single and many samples from the *citf1 spl7* double mutant did not contain detectible JA, we replaced the missing values with a value of the detection limit for the instrument, 1 ng/g fresh weight. JA concentrations in leaf tissues of different plant lines using the extraction procedure described by Wang et al. (2007) are shown in Supplemental Figure 7A.

Statistical Analysis

Statistical analyses of experimental data were performed using the ANOVA single-factor analysis and Student's *t* test using AnalysisToolPak of Microsoft Excel 2013. Statistical analysis of RT-qPCR data was performed using the Relative Expression Software Tool (REST; Pfaffl et al., 2002).

Accession Numbers

Sequence data for genes used in this study can be found in the GenBank/EMBL libraries under the following accession numbers: *CITF1* (AT1G71200), *SPL7* (AT5G18830), *COPT2* (AT3G46900), *FRO4* (AT5G23980), *FRO5* (AT5G23990), *LOX2* (AT3G45140), *LOX3* (AT1G17420), *LOX4* (AT1G72520), *DAD1* (AT2G44810), *OPR3* (AT2G06050), *AOC1* (AT3G25760), *AOC2* (AT3G25770), *AOC3* (AT3G25780), *KAT5* (AT5G48880), *REP1* (AT1G02340), *FSD1* (AT4G25100), *Pectin lyase-like* (AT1G48100), *CSD1* (AT1G08830), *CDS2* (AT2G28190), *NCED3* (AT3G14440), *EDL3* (AT3G63060), *CCS* (AT1G12520), *MATE* (AT1G33100), *CCT motif* (AT2G46670), *SDI1* (AT5G48850), and *IRT1* (AT4G19690). *CITF1* mutant alleles used in this study were SALK_073160 (*alias citf1*-1) and SAIL_711_B07 (*alias citf1*-2).

Supplemental Data

Supplemental Figure 1. JA biosynthesis pathway.

Supplemental Figure 2. Validation of RNA-seq results by RT-qPCR.

Supplemental Figure 3. CITF1 localizes to the nucleus.

Supplemental Figure 4. Characterization of *citf1* mutant alleles.

Supplemental Figure 5. The *citf1 spl7* double mutant has defects in the development of reproductive organs.

Supplemental Figure 6. SXRF analysis of Cu localization in flowers of wild-type and indicated Arabidopsis mutants.

Supplemental Figure 7. Exogenous JA application does not rescue the infertility of the *citf1 spl7* double mutant.

Supplemental Figure 8. In silico analyses of the effect of exogenously applied JA on the expression of some of Cu-responsive genes using the eFP browser (Winter et al., 2007).

Supplemental Table 1. Genes contributing to Cu sparing due to metabolome reorganization under Cu deficiency in flowers of Arabidopsis based on RNA-seq.

Supplemental Table 2. JA biosynthetic genes upregulated under Cu deficiency in flowers of Arabidopsis based on RNA-seq.

Supplemental Table 3. A list of used oligos.

Supplemental Data Set 1. Statistical analysis of the RNA-seq data.

Supplemental Data Set 2. Cu-responsive genes in flower buds of Arabidopsis.

Supplemental Data Set 3. Cu-responsive genes in mature flowers of Arabidopsis.

Supplemental Data Set 4. Cu-responsive transporter genes in flower buds of Arabidopsis based on RNA-seq.

Supplemental Data Set 5. Cu-responsive transporter genes in mature flowers of Arabidopsis based on RNA-seq.

Supplemental Data Set 6. Cu-responsive transcription factor genes in flower buds of Arabidopsis based on RNA-seq.

Supplemental Data Set 7. Cu-responsive transcription factor genes in mature flowers of Arabidopsis based on RNA-seq.

ACKNOWLEDGMENTS

We thank Ute Krämer (Ruhr University of Bochum, Germany), Roberto Solano (University of Madrid), and Anna Stepanova (North Carolina State) for the stimulating and helpful discussions on the manuscript. We thank Toshiharu Shikanai (Kyoto University, Japan) and E. Farmer (University of Lausanne, Switzerland) for providing seeds of the *spl7*-1 and *lox3 lox4* mutants, respectively. We thank Arthur Woll and Louisa Smieska (CHESS) for the discussion and assistance in configuring SXRF experiments. We thank Katalin Boroczky for assisting in LC-MS-based JA analysis at the Cornell Chemical Ecology Core Facility. We thank Bohan Liu (University of California Santa Cruz) for helping with generating customized Venn diagrams. Work in the O.K.V. lab was supported by NIFA/USDA Hatch under 2014-15-151 and the National Science Foundation (IOS-1656321). J.Y. was supported by the Henry Wu fund. L.V.K. is supported by a Canada Excellence Research Chair in Food Systems and Security. CHESS is supported by the NSF and NIH/NIGMS via NSF Award DMR-1332208.

AUTHOR CONTRIBUTIONS

J.Y., J.-C.C., and O.K.V. designed the experiments. J.Y., J.-C.C., H.S., H.J., T.-O.Z., E.J.C., and L.Z. performed the experiments. R.H. contributed to the execution and analysis of the SXRF experiments at CHESS. C.J. and Z.F. analyzed RNA-seq data. L.V.K. contributed to discussion on the manuscript and provided analytical tools for the manuscript. The manuscript was written by O.K.V. and J.Y. All authors analyzed the data and contributed constructive comments on the manuscript.

Received May 10, 2017; revised October 9, 2017; accepted November 3, 2017; published November 17, 2017.

REFERENCES

Abdel-Ghany, S.E., and Pilon, M. (2008). MicroRNA-mediated systemic down-regulation of copper protein expression in response to low copper availability in Arabidopsis. J. Biol. Chem. **283:** 15932–15945.

Alexander, M.P. (1969). Differential staining of aborted and non-aborted pollen. Stain Technol. **44:** 117–122.

Alonso, J.M., et al. (2003). Genome-wide insertional mutagenesis of *Arabidopsis thaliana*. Science **301:** 653–657.

Alvarez-Buylla, E.R., Benítez, M., Corvera-Poiré, A., Chaos Cador, A., de Folter, S., Gamboa de Buen, A., Garay-Arroyo, A., García-Ponce, B., Jaimes-Miranda, F., Pérez-Ruiz, R.V., Piñeyro-Nelson, A., and Sánchez-Corrales, Y.E. (2010). Flower development. Arabidopsis Book **8:** e0127.

Angulo, J.F., Rouer, E., Benarous, R., and Devoret, R. (1991). Identification of a mouse cDNA fragment whose expressed polypeptide reacts with anti-recA antibodies. Biochimie **73:** 251–256.

Attallah, C.V., Welchen, E., and Gonzalez, D.H. (2007). The promoters of *Arabidopsis thaliana* genes AtCOX17-1 and -2, encoding a copper chaperone involved in cytochrome c oxidase biogenesis, are preferentially active in roots and anthers and induced by biotic and abiotic stress. Physiol. Plant. **129:** 123–134.

Benjamini, Y., and Hochberg, Y. (1995). Controlling the false discovery rate: a practical and powerful approach to multiple testing. J. R. Stat. Soc. B Met. **57:** 289–300.

Bernal, M., Casero, D., Singh, V., Wilson, G.T., Grande, A., Yang, H., Dodani, S.C., Pellegrini, M., Huijser, P., Connolly, E.L., Merchant, S.S., and Krämer, U. (2012). Transcriptome sequencing identifies SPL7-regulated copper acquisition genes FRO4/FRO5 and the copper dependence of iron homeostasis in Arabidopsis. Plant Cell **24:** 738–761.

Birkenbihl, R.P., Jach, G., Saedler, H., and Huijser, P. (2005). Functional dissection of the plant-specific SBP-domain: overlap of the DNA-binding and nuclear localization domains. J. Mol. Biol. **352:** 585–596.

Blaby-Haas, C.E., and Merchant, S.S. (2017). Regulating cellular trace metal economy in algae. Curr. Opin. Plant Biol. **39:** 88–96.

Bock, K.W., Honys, D., Ward, J.M., Padmanaban, S., Nawrocki, E.P., Hirschi, K.D., Twell, D., and Sze, H. (2006). Integrating membrane transport with male gametophyte development and function through transcriptomics. Plant Physiol. **140:** 1151–1168.

Bolger, A.M., Lohse, M., and Usadel, B. (2014). Trimmomatic: a flexible trimmer for Illumina sequence data. Bioinformatics **30:** 2114–2120.

Boyle, E.I., Weng, S., Gollub, J., Jin, H., Botstein, D., Cherry, J.M., and Sherlock, G. (2004). GO:TermFinder–open source software for accessing Gene Ontology information and finding significantly enriched Gene Ontology terms associated with a list of genes. Bioinformatics **20:** 3710–3715.

Broadley, M., Brown, P., Cakmak, I., Rengel, Z., and Zhao, F. (2012). Function of nutrients: micronutrients. In Marschner's Mineral Nutrition of Higher Plants, 3rd ed, P. Marschner, ed (San Diego, CA: Academic Press), pp. 191–248.

Browse, J. (2009). Jasmonate passes muster: a receptor and targets for the defense hormone. Annu. Rev. Plant Biol. **60:** 183–205.

Burkhead, J.L., Reynolds, K.A., Abdel-Ghany, S.E., Cohu, C.M., and Pilon, M. (2009). Copper homeostasis. New Phytol. **182:** 799–816.

Caldelari, D., Wang, G., Farmer, E.E., and Dong, X. (2011). Arabidopsis lox3 lox4 double mutants are male sterile and defective in global proliferative arrest. Plant Mol. Biol. **75:** 25–33.

Cecchetti, V., Altamura, M.M., Falasca, G., Costantino, P., and Cardarelli, M. (2008). Auxin regulates Arabidopsis anther dehiscence, pollen maturation, and filament elongation. Plant Cell **20:** 1760–1774.

Chen, H., and Boutros, P.C. (2011). VennDiagram: a package for the generation of highly-customizable Venn and Euler diagrams in R. BMC Bioinformatics **12:** 35.

Cheng, H., Qin, L., Lee, S., Fu, X., Richards, D.E., Cao, D., Luo, D., Harberd, N.P., and Peng, J. (2004). Gibberellin regulates Arabidopsis floral development via suppression of DELLA protein function. Development **131:** 1055–1064.

Chu, H.-H., Chiecko, J., Punshon, T., Lanzirotti, A., Lahner, B., Salt, D.E., and Walker, E.L. (2010). Successful reproduction requires the function of Arabidopsis Yellow Stripe-Like1 and Yellow Stripe-Like3 metal-nicotianamine transporters in both vegetative and reproductive structures. Plant Physiol. **154:** 197–210.

Chung, S.M., Frankman, E.L., and Tzfira, T. (2005). A versatile vector system for multiple gene expression in plants. Trends Plant Sci. **10:** 357–361.

Clough, S.J., and Bent, A.F. (1998). Floral dip: a simplified method for Agrobacterium-mediated transformation of *Arabidopsis thaliana*. Plant J. **16:** 735–743.

Colangelo, E.P., and Guerinot, M.L. (2004). The essential basic helix-loop-helix protein FIT1 is required for the iron deficiency response. Plant Cell **16:** 3400–3412.

Daughety, M.M., and DeLoughery, T.G. (2017). Unusual anemias. Med. Clin. North Am. **101:** 417–429.

DiDonato, R.J., Jr., Roberts, L.A., Sanderson, T., Eisley, R.B., and Walker, E.L. (2004). Arabidopsis Yellow Stripe-Like2 (YSL2): a metal-regulated gene encoding a plasma membrane transporter of nicotianamine-metal complexes. Plant J. **39:** 403–414.

Donner, E., Punshon, T., Guerinot, M.L., and Lombi, E. (2012). Functional characterisation of metal(loid) processes in planta through the integration of synchrotron techniques and plant molecular biology. Anal. Bioanal. Chem. **402:** 3287–3298.

Einsle O, Mehrabian Z, Nalbandyan R, and Messerschmidt A (2000). Crystal structure of plantacyanin, a basic blue cupredoxin from spinach. J. Biol. Inorg. Chem. **5:** 666–672.

Endo, M., Tsuchiya, T., Hamada, K., Kawamura, S., Yano, K., Ohshima, M., Higashitani, A., Watanabe, M., and Kawagishi-Kobayashi, M. (2009). High temperatures cause male sterility in rice plants with transcriptional alterations during pollen development. Plant Cell Physiol. **50:** 1911–1922.

Feys, B., Benedetti, C.E., Penfold, C.N., and Turner, J.G. (1994). Arabidopsis mutants selected for resistance to the phytotoxin coronatine are male sterile, insensitive to methyl jasmonate, and resistant to a bacterial pathogen. Plant Cell **6:** 751–759.

Fonseca, S., Chico, J.M., and Solano, R. (2009a). The jasmonate pathway: the ligand, the receptor and the core signalling module. Curr. Opin. Plant Biol. **12:** 539–547.

Fonseca, S., Chini, A., Hamberg, M., Adie, B., Porzel, A., Kramell, R., Miersch, O., Wasternack, C., and Solano, R. (2009b). (+)-7-iso-Jasmonoyl-L-isoleucine is the endogenous bioactive jasmonate. Nat. Chem. Biol. **5:** 344–350.

Garcia-Molina, A., Xing, S., and Huijser, P. (2014). A conserved KIN17 curved DNA-binding domain protein assembles with SQUAMOSA PROMOTER-BINDING PROTEIN-LIKE7 to adapt Arabidopsis growth and development to limiting copper availability. Plant Physiol. **164:** 828–840.

Gayomba, S.R., Jung, H.I., Yan, J., Danku, J., Rutzke, M.A., Bernal, M., Krämer, U., Kochian, L.V., Salt, D.E., and Vatamaniuk, O.K. (2013). The CTR/COPT-dependent copper uptake and SPL7-dependent copper deficiency responses are required for basal cadmium tolerance in *A. thaliana.* Metallomics **5:** 1262–1275.

He, Y., Fukushige, H., Hildebrand, D.F., and Gan, S. (2002). Evidence supporting a role of jasmonic acid in Arabidopsis leaf senescence. Plant Physiol. **128:** 876–884.

Himelblau, E., and Amasino, R.M. (2001). Nutrients mobilized from leaves of *Arabidopsis thaliana* during leaf senescence. J. Plant Physiol. **158:** 1317–1323.

Himelblau, E., Mira, H., Lin, S.-J., Culotta, V.C., Peñarrubia, L., and Amasino, R.M. (1998). Identification of a functional homolog of the yeast copper homeostasis gene ATX1 from Arabidopsis. Plant Physiol. **117:** 1227–1234.

Ishiguro, S., Kawai-Oda, A., Ueda, J., Nishida, I., and Okada, K. (2001). The DEFECTIVE IN ANTHER DEHISCIENCE gene encodes a novel phospholipase A1 catalyzing the initial step of jasmonic acid biosynthesis, which synchronizes pollen maturation, anther dehiscence, and flower opening in Arabidopsis. Plant Cell **13:** 2191–2209.

Jain, A., Wilson, G.T., and Connolly, E.L. (2014). The diverse roles of FRO family metalloreductases in iron and copper homeostasis. Front. Plant Sci. **5:** 100.

Jung, H.I., Gayomba, S.R., Rutzke, M.A., Craft, E., Kochian, L.V., and Vatamaniuk, O.K. (2012). COPT6 is a plasma membrane transporter that functions in copper homeostasis in *Arabidopsis* and is a novel target of SQUAMOSA promoter-binding protein-like 7. J. Biol. Chem. **287:** 33252–33267.

Kapuscinski, J. (1995). DAPI: a DNA-specific fluorescent probe. Biotech. Histochem. **70:** 220–233.

Kobayashi, T., Itai, R.N., Senoura, T., Oikawa, T., Ishimaru, Y., Ueda, M., Nakanishi, H., and Nishizawa, N.K. (2016). Jasmonate signaling is activated in the very early stages of iron deficiency responses in rice roots. Plant Mol. Biol. **91:** 533–547.

Kombrink, E. (2012). Chemical and genetic exploration of jasmonate biosynthesis and signaling paths. Planta **236:** 1351–1366.

Kropat, J., Gallaher, S.D., Urzica, E.I., Nakamoto, S.S., Strenkert, D., Tottey, S., Mason, A.Z., and Merchant, S.S. (2015). Copper economy in Chlamydomonas: prioritized allocation and reallocation of copper to respiration vs. photosynthesis. Proc. Natl. Acad. Sci. USA **112:** 2644–2651.

Kropat, J., Tottey, S., Birkenbihl, R.P., Depège, N., Huijser, P., and Merchant, S. (2005). A regulator of nutritional copper signaling in Chlamydomonas is an SBP domain protein that recognizes the GTAC core of copper response element. Proc. Natl. Acad. Sci. USA **102:** 18730–18735.

Langmead, B., Trapnell, C., Pop, M., and Salzberg, S.L. (2009). Ultrafast and memory-efficient alignment of short DNA sequences to the human genome. Genome Biol. **10:** R25.

Llanos, R.M., and Mercer, J.F. (2002). The molecular basis of copper homeostasis copper-related disorders. DNA Cell Biol. **21:** 259–270.

McCaig, B.C., Meagher, R.B., and Dean, J.F.D. (2005). Gene structure and molecular analysis of the laccase-like multicopper oxidase (LMCO) gene family in *Arabidopsis thaliana*. Planta **221:** 619–636.

McConn, M., and Browse, J. (1996). The critical requirement for linolenic acid is pollen development, not photosynthesis, in an Arabidopsis mutant. Plant Cell **8:** 403–416.

Mendel, R.R., and Kruse, T. (2012). Cell biology of molybdenum in plants and humans. Biochim. Biophys. Acta **1823:** 1568–1579.

Mira, H., Martínez-García, F., and Peñarrubia, L. (2001). Evidence for the plant-specific intercellular transport of the Arabidopsis copper chaperone CCH. Plant J. **25:** 521–528.

Murashige, T., and Skoog, F. (1962). A revised medium for rapid growth and biological assays with tobacco tissue cultures. Physiol. Plant. **15:** 473–497.

Park, J.-H., Halitschke, R., Kim, H.B., Baldwin, I.T., Feldmann, K.A., and Feyereisen, R. (2002). A knock-out mutation in allene oxide synthase results in male sterility and defective wound signal transduction in Arabidopsis due to a block in jasmonic acid biosynthesis. Plant J. **31:** 1–12.

Pfaffl, M.W., Horgan, G.W., and Dempfle, L. (2002). Relative expression software tool (REST) for group-wise comparison and statistical analysis of relative expression results in real-time PCR. Nucleic Acids Res. **30:** e36.

Pilon, M. (2017). The copper microRNAs. New Phytol. **213:** 1030–1035.

Printz, B., Lutts, S., Hausman, J.-F., and Sergeant, K. (2016). Copper trafficking in plants and its implication on cell wall dynamics. Front. Plant Sci. **7:** 601.

Quast, C., Pruesse, E., Yilmaz, P., Gerken, J., Schweer, T., Yarza, P., Peplies, J., and Glöckner, F.O. (2013). The SILVA ribosomal RNA gene database project: improved data processing and web-based tools. Nucleic Acids Res. **41:** D590–D596.

Quinn, J.M., Barraco, P., Eriksson, M., and Merchant, S. (2000). Coordinate copper- and oxygen-responsive Cyc6 and Cpx1 expression in Chlamydomonas is mediated by the same element. J. Biol. Chem. **275:** 6080–6089.

Rapisarda, V.A., Volentini, S.I., Farías, R.N., and Massa, E.M. (2002). Quenching of bathocuproine disulfonate fluorescence by Cu(I) as a basis for copper quantification. Anal. Biochem. **307:** 105–109.

Ravet, K., Danford, F.L., Dihle, A., Pittarello, M., and Pilon, M. (2011). Spatiotemporal analysis of copper homeostasis in *Populus trichocarpa* reveals an integrated molecular remodeling for a preferential allocation of copper to plastocyanin in the chloroplasts of developing leaves. Plant Physiol. **157:** 1300–1312.

Ravet, K., and Pilon, M. (2013). Copper and iron homeostasis in plants: the challenges of oxidative stress. Antioxid. Redox Signal. **19:** 919–932.

Robinson, M.D., McCarthy, D.J., and Smyth, G.K. (2010). edgeR: a Bioconductor package for differential expression analysis of digital gene expression data. Bioinformatics **26:** 139–140.

Rydén, L.G., and Hunt, L.T. (1993). Evolution of protein complexity: the blue copper-containing oxidases and related proteins. J. Mol. Evol. **36:** 41–66.

Sancenón, V., Puig, S., Mateu-Andrés, I., Dorcey, E., Thiele, D.J., and Peñarrubia, L. (2004). The Arabidopsis copper transporter COPT1 functions in root elongation and pollen development. J. Biol. Chem. **279:** 15348–15355.

Sanders, P.M., Bui, A.Q., Weterings, K., McIntire, K.N., Hsu, Y.-C., Lee, P.Y., and Goldberg, R.B. (1999). Anther developmental defects in *Arabidopsis thaliana* male-sterile mutants. Sex. Plant Reprod. **11:** 297–322.

Schilmiller, A.L., Koo, A.J.K., and Howe, G.A. (2007). Functional diversification of acyl-coenzyme A oxidases in jasmonic acid biosynthesis and action. Plant Physiol. **143:** 812–824.

Scott, R.J., Spielman, M., and Dickinson, H.G. (2004). Stamen structure and function. Plant Cell **16** (Suppl): S46–S60.

Shahbaz, M., Ravet, K., Peers, G., and Pilon, M. (2015). Prioritization of copper for the use in photosynthetic electron transport in developing leaves of hybrid poplar. Front. Plant Sci. **6:** 407.

Sheard, L.B., et al. (2010). Jasmonate perception by inositol-phosphate-potentiated COI1-JAZ co-receptor. Nature **468:** 400–405.

Shorrocks, V.M., and Alloway, B.J. (1988). Copper in Plant, Animal and Human Nutrition. (Potters Bar, Hertfordshire, UK: Copper Development Association).

Smith, A.R., and Zhao, D. (2016). Sterility caused by floral organ degeneration and abiotic stresses in Arabidopsis and cereal grains. Front. Plant Sci. **7:** 1503.

Solé, V.A., Papillon, E., Cotte, M., Walter, P., and Susini, J. (2007). A multiplatform code for the analysis of energy-dispersive X-ray fluorescence spectra. Spectrochim. Acta Part B At. Spectrosc. **62:** 63–68.

Sommer, F., Kropat, J., Malasarn, D., Grossoehme, N.E., Chen, X., Giedroc, D.P., and Merchant, S.S. (2010). The CRR1 nutritional copper sensor in Chlamydomonas contains two distinct metal-responsive domains. Plant Cell **22:** 4098–4113.

Song, S., Qi, T., Huang, H., and Xie, D. (2013). Regulation of stamen development by coordinated actions of jasmonate, auxin, and gibberellin in Arabidopsis. Mol. Plant **6:** 1065–1073.

Staswick, P.E., Tiryaki, I., and Rowe, M.L. (2002). Jasmonate response locus JAR1 and several related Arabidopsis genes encode enzymes of the firefly luciferase superfamily that show activity on jasmonic, salicylic, and indole-3-acetic acids in an assay for adenylation. Plant Cell **14:** 1405–1415.

Stintzi, A., and Browse, J. (2000). The Arabidopsis male-sterile mutant, opr3, lacks the 12-oxophytodienoic acid reductase required for jasmonate synthesis. Proc. Natl. Acad. Sci. USA **97:** 10625–10630.

Tchieu, J.H., Fana, F., Fink, J.L., Harper, J., Nair, T.M., Niedner, R.H., Smith, D.W., Steube, K., Tam, T.M., Veretnik, S., Wang, D., and Gribskov, M. (2003). The PlantsP and PlantsT functional genomics databases. Nucleic Acids Res. **31:** 342–344.

Trapnell, C., Pachter, L., and Salzberg, S.L. (2009). TopHat: discovering splice junctions with RNA-Seq. Bioinformatics **25:** 1105–1111.

von Malek, B., van der Graaff, E., Schneitz, K., and Keller, B. (2002). The Arabidopsis male-sterile mutant dde2-2 is defective in the ALLENE OXIDE SYNTHASE gene encoding one of the key enzymes of the jasmonic acid biosynthesis pathway. Planta **216:** 187–192.

Wang, L., Halitschke, R., Kang, J.H., Berg, A., Harnisch, F., and Baldwin, I.T. (2007). Independently silencing two JAR family members impairs levels of trypsin proteinase inhibitors but not nicotine. Planta **226:** 159–167.

Wasternack, C., and Hause, B. (2013). Jasmonates: biosynthesis, perception, signal transduction and action in plant stress response, growth and development. An update to the 2007 review in Annals of Botany. Ann. Bot. **111:** 1021–1058.

Waters, B.M., Chu, H.H., Didonato, R.J., Roberts, L.A., Eisley, R.B., Lahner, B., Salt, D.E., and Walker, E.L. (2006). Mutations in Arabidopsis yellow stripe-like1 and yellow stripe-like3 reveal their roles in metal ion homeostasis and loading of metal ions in seeds. Plant Physiol. **141:** 1446–1458.

Winter, D., Vinegar, B., Nahal, H., Ammar, R., Wilson, G.V., and Provart, N.J. (2007). An "Electronic Fluorescent Pictograph" browser for exploring and analyzing large-scale biological data sets. PLoS One **2:** e718.

Yamasaki, H., Hayashi, M., Fukazawa, M., Kobayashi, Y., and Shikanai, T. (2009). SQUAMOSA Promoter Binding Protein-Like7 is a central regulator for copper homeostasis in *Arabidopsis.* Plant Cell **21:** 347–361.

Yan, J., Li, S., Gu, M., Yao, R., Li, Y., Chen, J., Yang, M., Tong, J., Xiao, L., Nan, F., and Xie, D. (2016). Endogenous bioactive jasmonate is composed of a set of (+)-7-iso-JA-amino acid conjugates. Plant Physiol. **172:** 2154–2164.

Yuan, Z., and Zhang, D. (2015). Roles of jasmonate signalling in plant inflorescence and flower development. Curr. Opin. Plant Biol. **27:** 44–51.

Zhai, Z., et al. (2014). OPT3 is a phloem-specific iron transporter that is essential for systemic iron signaling and redistribution of iron and cadmium in Arabidopsis. Plant Cell **26:** 2249–2264.

Zhai, Z., Jung, H.I., and Vatamaniuk, O.K. (2009). Isolation of protoplasts from tissues of 14-day-old seedlings of *Arabidopsis thaliana*. J. Vis. Exp. **pii:** 1149.

Zheng, Y., et al. (2016). iTAK: a program for genome-wide prediction and classification of plant transcription factors, transcriptional regulators, and protein kinases. Mol. Plant **9:** 1667–1670.

Zhong, S., Joung, J.G., Zheng, Y., Chen, Y.R., Liu, B., Shao, Y., Xiang, J.Z., Fei, Z., and Giovannoni, J.J. (2011). High-throughput Illumina strand-specific RNA sequencing library preparation. Cold Spring Harb. Protoc. **2011:** 940–949.